

Signals From the Epoch of Cosmological Recombination (*Karl Schwarzschild Lecture*)

R.A. Sunyaev^{1,2} and J. Chluba^{3,1}

¹ Max-Planck-Institut für Astrophysik, Karl-Schwarzschild-Str. 1, 85741 Garching, Germany

² Space Research Institute, Russian Academy of Sciences, Profsoyuznaya 84/32, 117997 Moscow, Russia

³ Canadian Institute for Theoretical Astrophysics, 60 St. George Street, Toronto, ON M5S 3H8, Canada

October 29, 2018

Abstract

The physical ingredients to describe the epoch of cosmological recombination are amazingly simple and well-understood. This fact allows us to take into account a very large variety of physical processes, still finding potentially measurable consequences for the *energy spectrum* and *temperature anisotropies* of the Cosmic Microwave Background (CMB). In this contribution we provide a short historical overview in connection with the cosmological recombination epoch and its connection to the CMB. Also we highlight some of the detailed physics that were studied over the past few years in the context of the cosmological recombination of *hydrogen* and *helium*.

The impact of these considerations is two-fold: (i) the associated release of photons during this epoch leads to interesting and *unique deviations* of the Cosmic Microwave Background (CMB) energy spectrum *from a perfect blackbody*, which, in particular at decimeter wavelength and the Wien part of the CMB spectrum, may become observable in the near future. Despite the fact that the abundance of helium is rather small, it still contributes a sizeable amount of photons to the full recombination spectrum, leading to additional distinct spectral features. Observing the spectral distortions from the epochs of hydrogen and helium recombination, in principle would provide an additional way to determine some of the key parameters of the Universe (e.g. the specific entropy, the CMB monopole temperature and the pre-stellar abundance of helium). Also it permits us to confront our detailed understanding of the recombination process with *direct observational evidence*. In this contribution we illustrate how the theoretical *spectral template* of the cosmological recombination spectrum may be utilized for this purpose. We also show that because hydrogen and helium recombine at very different epochs it is possible to address questions related to the *thermal history* of our Universe. In particular the cosmological recombination radiation may allow us to distinguish between Compton γ -distortions that were created by energy release *before* or *after* the recombination of the Universe finished.

(ii) with the advent of high precision CMB data, e.g. as will be available using the PLANCK Surveyor or CMBPOL, a very accurate theoretical understanding of the *ionization history* of the Universe becomes necessary for the interpretation of the CMB temperature and polarization anisotropies. Here we show that the uncertainty in the ionization history due to several processes, which until now were not taken in to account in the standard recombination code RECFAST, reaches the percent level. In particular $\text{He II} \rightarrow \text{He I}$ -recombination occurs significantly faster because of the presence of a tiny fraction of neutral hydrogen at $z \lesssim 2400$. Also recently it was demonstrated that in the case of H I Lyman α photons the *time-dependence* of the emission process and the *asymmetry* between the emission and absorption profile cannot be ignored. However, it is indeed surprising how *inert* the cosmological recombination history is even at percent-level accuracy. Observing the cosmological recombination spectrum should in principle allow us to directly check this conclusion, which until now is purely theoretical. Also it may allow to *reconstruct the ionization history* using observational data.

1 Introduction

The Gunn-Peterson effect demonstrated clearly that intergalactic gas is strongly ionized in our vicinity till at least redshift $z \sim 6.5$. We are sure that at very high redshifts $z \gg 1000$ the CMB temperature was so high that hydrogen in the primordial matter should be completely ionized (see Fig 1). Today we have no doubts that Universe was practically neutral at redshifts $20 \lesssim z \lesssim 1000$. The periods of *reionization* (connected with formation of first stars and enormously strong release of UV-radiation) and of *cosmological hydrogen recombination* at redshift ~ 1000 are of special importance for modern cosmology because they permit us to collect a lot of information about *history*, *structure* and *key parameters* of our Universe.

What is so beautiful about cosmological recombination?

Within the cosmological concordance model the physical environment during the epoch of cosmological recombination (redshifts $500 \lesssim z \lesssim 2000$ for hydrogen, $1600 \lesssim z \lesssim 3500$ for $\text{He II} \rightarrow \text{He I}$ and $5000 \lesssim z \lesssim 8000$ for $\text{He III} \rightarrow \text{He II}$ recombination; also see Fig. 1) is extremely simple: the Universe is homogeneous and isotropic, globally neutral and is expanding at a rate that can be computed knowing a small set of cosmological parameters. The baryonic matter component is dominated by hydrogen ($\sim 76\%$) and helium ($\sim 24\%$), with negligibly small traces of other light elements, such as deuterium and lithium, and it is continuously exposed to a bath of isotropic blackbody radiation, which contains roughly 1.6×10^9 photons per baryon.

At redshift $z \sim 1400$ the electron number density in the Universe was close to $N_e \sim 500 \text{ cm}^{-3}$, a value that is not very far from the densities of many compact H II regions in our Galaxy. However, what makes the situation drastically different from the one in ionized nebulae is the *ambient bath of CMB photons* with the same temperature as electrons, $T_e = T_\gamma \sim 3815 \text{ K}$, and the huge photon number density $N_\gamma \sim 1.1 \times 10^{12} \text{ cm}^{-3}$. In contrast to H II regions, radiative processes (instead of collisional processes and the interaction with strongly diluted stellar UV radiation spec-

trum) are most important. Furthermore, there are no heavy elements and dust. It is these conditions that make stimulated radiative processes, photoabsorption and ionization play an especially important role during hydrogen recombination. Another principle difference is the transition from problems with a spatial boundary in H II regions to the practically uniform Universe without boundaries. Therefore the evolution of radiation in the expanding Universe is connected with a *time-dependent* rather than a *spatial* problem.

These initially simple and very unique settings in principle allow us to predict the *ionization history* of the Universe and the *cosmological recombination spectrum* (see Sects. 2) with extremely high accuracy, where the limitations are mainly set by our understanding of the *atomic processes* and associated transition rates. In particular for neutral helium our knowledge is still rather poor. Only very recently highly accurate and user-friendly tables for the main transitions and energies of levels with $n \leq 10$ have been published (Drake & Morton, 2007), but there is no principle difficulty in extending these to larger n (Beigman & Vainshtein, 2009). Also the data regarding the photo-ionization cross sections of neutral helium should be updated and extended.

In any case, it is this simplicity that offers us the possibility to enter a rich field of physical processes and to challenge our understanding of atomic physics, radiative transfer and cosmology, eventually leading to a *beautiful* variety of potentially observable effects in connection with the CMB radiation.

What is so special about cosmological recombination?

The main reason for the described simplicity is the *extremely large specific entropy* and the *slow expansion* of our Universe. Because of the huge number of CMB photons, the free electrons are tightly coupled to the radiation field due to tiny energy exchange during *Compton scattering* off thermal electrons until rather low redshifts, such that during recombination the thermodynamic temperature of electrons is equal to the CMB blackbody temperature with very high precision. Without this strong interaction between photons and electrons the temperature of the electrons would scale like $T_e \propto (1+z)^2$, while the temperature of the photon field drops like $T_\gamma \propto (1+z)$. In addition, the very fast *Coulomb interaction* and atom-ion collisions allows to maintain full thermodynamic equilibrium among the electrons, ions and neutral atoms down to $z \sim 150$ (Zeldovich et al., 1968). It is only below this redshift that the matter temperature starts to drop faster than the radiation temperature, a fact that is also very important in connection with the 21 cm signals coming from high redshift before the Universe got reionized at $z \sim 10$ (Madau et al., 1997). Furthermore, processes in the baryonic sector cannot severely affect any of the radiation properties, down to redshift where the first stars and galaxies appear, so that as mentioned above the atomic rates are largely dominated by radiative processes, including *stimulated recombination*, *induced emission* and absorption of photons. On the other hand, the slow expansion of the Universe allows us to consider the evolution of the atomic species along a sequence of *quasi-stationary* stages, where the populations of the levels are nearly in full equilibrium with the radiation field, but only subsequently and very slowly drop out of equilibrium, finally leading to *recombination* and the *release of additional photons* in uncompensated bound-bound and free-bound transitions.

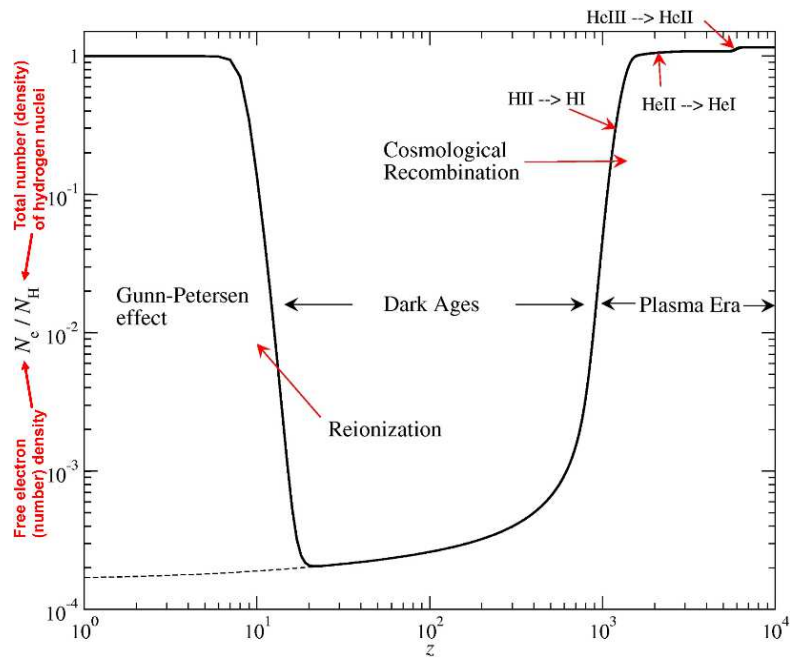


Figure 1: Sketch of the cosmological ionization history as a function of redshift z . At high redshift the Universe was completely ionized. As it expanded and cooled down it went through several stages of recombination, starting with He III \rightarrow He II recombination ($z \sim 7000$), He II \rightarrow He I recombination ($z \sim 2500$), and ending with the recombination of hydrogen ($z \sim 1000$). At low redshift ($z \lesssim 10$) the Universe eventually gets re-ionized by the first sources of radiation that appear in the Universe.



Figure 2: Yakov B. Zeldovich (top), Vladimir Kurt (lower left) and RS (lower right).

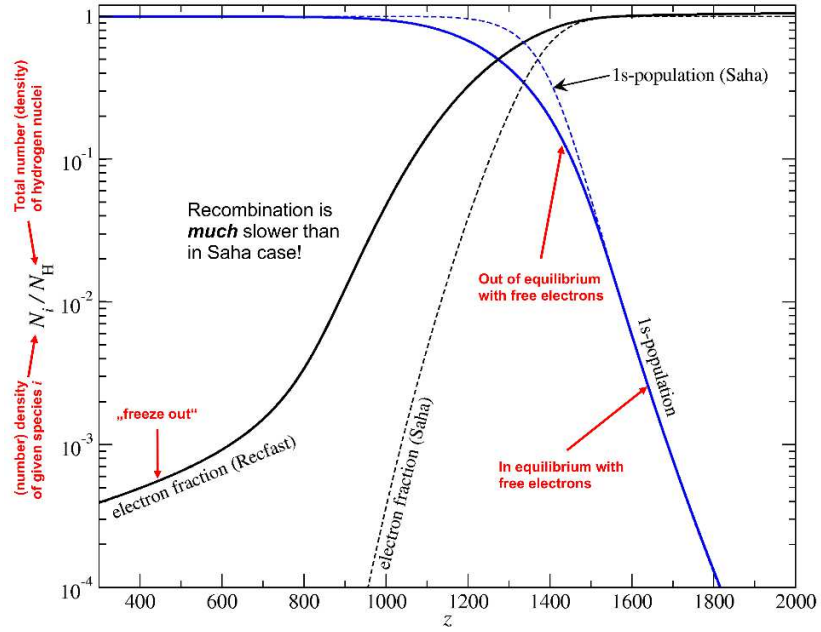


Figure 3: Illustration of the difference in the hydrogen recombination history in comparison with the Saha case. The recombination of hydrogen in the Universe is strongly delayed due to the 'bottleneck' created in the Lyman α resonance and the slow 2s-1s two-photon transition.



Figure 4: Viktor Dubrovich.

Brief historical overview for hydrogen recombination

It was realized at the end of the 60's (Zeldovich et al., 1968; Peebles, 1968), that during the epoch of cosmological hydrogen recombination (typical redshifts $800 \lesssim z \lesssim 1600$) any direct recombination of electrons to the ground state of hydrogen is immediately followed by the ionization of a neighboring neutral atom due to re-absorption of the newly released Lyman-continuum photon. In addition, because of the enormous difference in the $2p \leftrightarrow 1s$ dipole transition rate and the Hubble expansion rate, photons emitted close to the center of the Lyman- α line scatter $\sim 10^7 - 10^8$ times before they can finally escape further interaction with the medium and thereby permit a successful settling of electrons in the $1s$ -level. It is due to these very peculiar circumstances that the $2s \leftrightarrow 1s$ -two-photon decay process (transition rate $A_{2s1s} \sim 8.22 \text{ s}^{-1}$), being about 8 orders of magnitude slower than the Lyman- α resonance transition, is able to substantially control the dynamics of cosmological hydrogen recombination (Zeldovich et al., 1968; Peebles, 1968), allowing about 57% of all hydrogen atoms in the Universe to recombine at redshift $z \lesssim 1400$ through this channel (Chluba & RS, 2006b).

Shortly afterwards (RS & Zeldovich, 1970a; Peebles & Yu, 1970) it became clear that the ionization history is one of the key ingredients for the theoretical predictions of the Cosmic Microwave Background (CMB) temperature and polarization anisotropies. Today these tiny directional variations of the CMB temperature ($\Delta T/T_0 \sim 10^{-5}$) around the mean value $T_0 = 2.725 \pm 0.001 \text{ K}$ (Fixsen & Mather, 2002) have been observed for the whole sky using the COBE and WMAP satellites, beyond doubt with great success. The high quality data coming from balloon-borne and ground-based CMB experiments (BOOMERANG, MAXIMA, ARCHEOPS, CBI, DASI and VSA etc.) today certainly provides one of the major pillars for the *cosmological concordance model* (Bahcall et al., 1999; Bennett et al., 2003). Very recently the PLANCK Surveyor was successfully launched and is now on its way to the L2 point, from which it will start observing the CMB with unprecedented precision very soon, further helping to establish the *era of precision cosmology*.

Radiation from the cosmological recombination epoch

In September 1966, one of the authors (RS) was explaining during a seminar at the Shternberg Astronomical Institute in Moscow how recombination should occur according to the Saha formula for equilibrium ionization. After the talk his friend (UV astronomer) *Vladimir Kurt* (see Fig. 2) asked him: '*but where are all the redshifted Lyman- α photons that were released during recombination?*' Indeed this was a great question, which was then addressed in detail by Zeldovich et al. (1968), leading to an understanding of the role of the $2s$ -two-photon decay, the delay of recombination as compared to the Saha-solution (see Fig. 3 for illustration), the spectral distortions of the CMB due to two-photon continuum and Lyman- α emission, the frozen remnant of ionized atoms, and the radiation and matter temperature equality until $z \sim 150$.

All recombined electrons in hydrogen lead to the release of $\sim 13.6 \text{ eV}$ in form of photons, but due to the large specific entropy of the Universe this will only add some fraction of $\Delta\rho_\gamma/\rho_\gamma \sim 10^{-9} - 10^{-8}$ to the total energy density of the CMB spectrum, and hence the corresponding distortions are expected to be very small. However, all

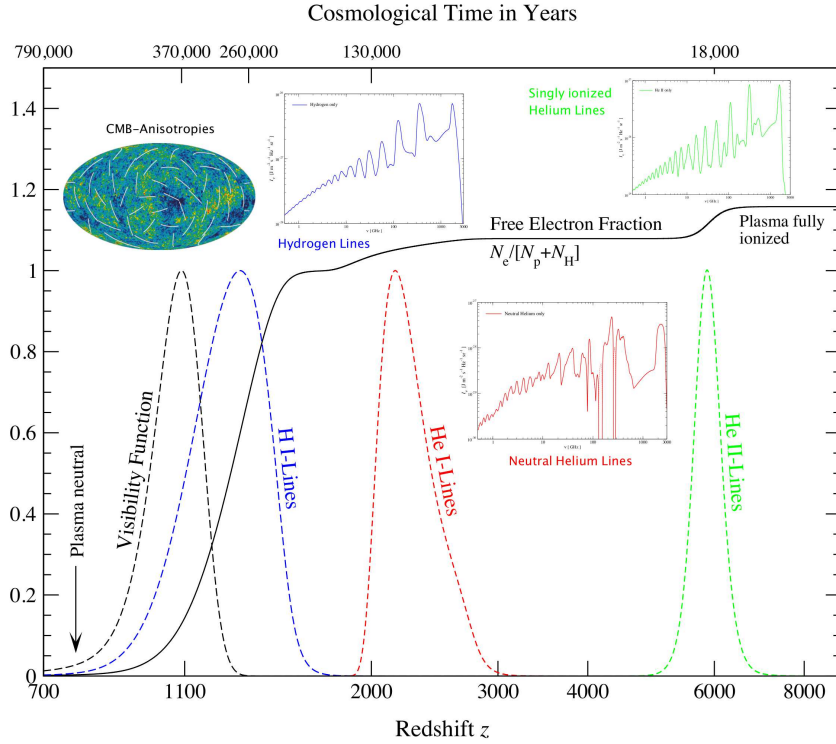


Figure 5: Ionization history of the Universe (solid black curve) and the origin of different CMB signals (dashed lines and inlays). The observed temperature anisotropies in the CMB temperature are created close to the maximum of the Thomson visibility function around $z \sim 1089$, whereas the direct information carried by the photons in the cosmological hydrogen recombination spectrum is from slightly earlier times. The photons associated with the *two* recombinations of helium were released at even higher redshifts. Finding the traces of these signals in the cosmological recombination spectrum will therefore allow us to learn about the state of the Universe at $\sim 130,000$ yrs and $\sim 18,000$ yrs after the big bang. Furthermore, the cosmological recombination radiation may offer a way to tell if something unexpected (e.g. energy release due to annihilating dark matter particles) occurred *before* the end of cosmological recombination.

the photons connected with the Lyman- α transition and the 2s-two-photon continuum appear in the Wien part of the CMB spectrum today, where the number of photons in the CMB blackbody is dropping exponentially, and, as realized earlier (Zeldovich et al., 1968; Peebles, 1968), these distortions are significant (see Sect. 2).

In 1975, *Victor Dubrovich* (see Fig. 4) pointed out that the transitions among highly excited levels in hydrogen are producing additional photons, which after redshifting are reaching us in the cm- and dm-spectral band. This band is actually accessible from the ground. Later these early estimates were significantly refined by several groups (e.g. see Kholupenko et al. (2005) and Rubiño-Martín et al. (2006) for references), with the most recent calculation performed by Chluba & RS (2006b), also including the previously neglected free-bound component, and showing in detail that the relative distortions are becoming more significant in the decimeter Rayleigh-Jeans part of the CMB blackbody spectrum (see Sects. 2, Fig. 8). These kind of precise computations are becoming feasible today, because (i) our knowledge of atomic data (in particular for neutral helium) has significantly improved; (ii) it is now possible to handle large systems of strongly coupled differential equations using modern computers; and (iii) we now know the cosmology model (and most the important parameters like Ω_b , T_γ and Hubble constant) with sufficiently high precision.

The most interesting aspect of this radiation is that it has a very *peculiar* but *well-defined, quasi-periodic spectral dependence*, where the photons emitted due to transitions between levels in the hydrogen atom are coming from redshifts $z \sim 1300 - 1400$, i.e. *before* the time of the formation of the CMB temperature anisotropies close to the maximum of the Thomson visibility function (see Fig. 5). Therefore, measuring these distortions of the CMB spectrum would provide a way to confront our understanding of the recombination epoch with *direct experimental evidence*, and in principle may open another independent way to determine some of the key parameters of the Universe, like the value of the CMB monopole temperature, T_0 , the number density of baryons, $\propto \Omega_b h^2$, or alternatively the specific entropy, and the primordial helium abundance (e.g. see Chluba & RS (2008a) and references therein).

Growth of adiabatic density perturbations in the Universe and baryonic acoustic oscillations

It is well known since the classical paper of Eugene Lifshitz in 1946 how adiabatic perturbations are growing in the Universe according to Einstein's theory of general relativity (GR). Nevertheless, it is possible to explain this process using a simple Newtonian approach and remembering the properties of Jeans gravitational instability. At sufficiently early times (but after inflation), when practically any scale of astronomical significance was bigger than the horizon ct (see upper panel in Fig. 6). any two different regions of the Universe were completely independent. If the densities within them were different, these independent universes expanded at different rates and the density differences (perturbations!) were growing according to a power law. The situation changed completely when the perturbation at a given scale became smaller than the horizon. At redshift $z \gtrsim 3300$ our Universe was radiation dominated: the radiation energy density ϵ_r and radiation pressure $\frac{1}{3} \epsilon_r \approx 0.91 N_\gamma k T_\gamma$ significantly exceeded $\epsilon_b = \rho_b c^2$ and the

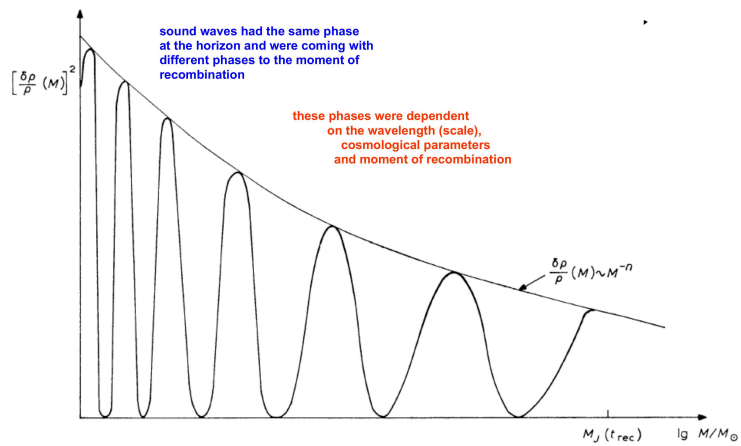
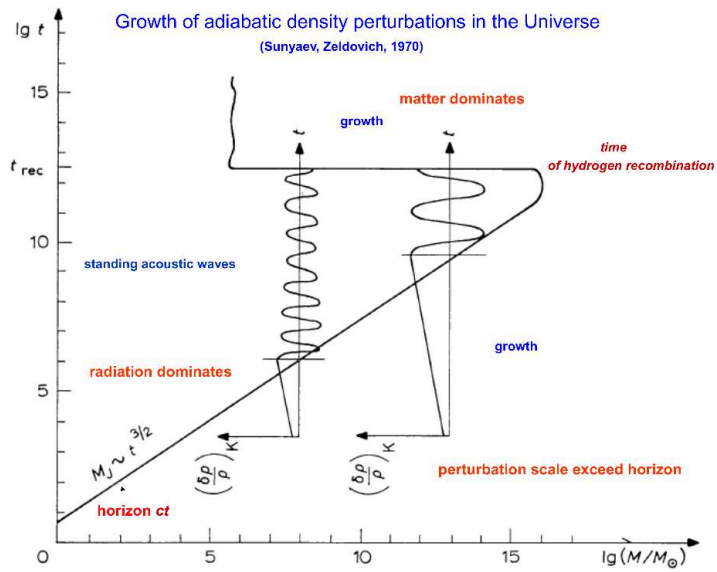


Figure 6: Illustration for the growth of adiabatic density perturbations in the Universe. The figure was adapted from RS & Zeldovich (1970a).

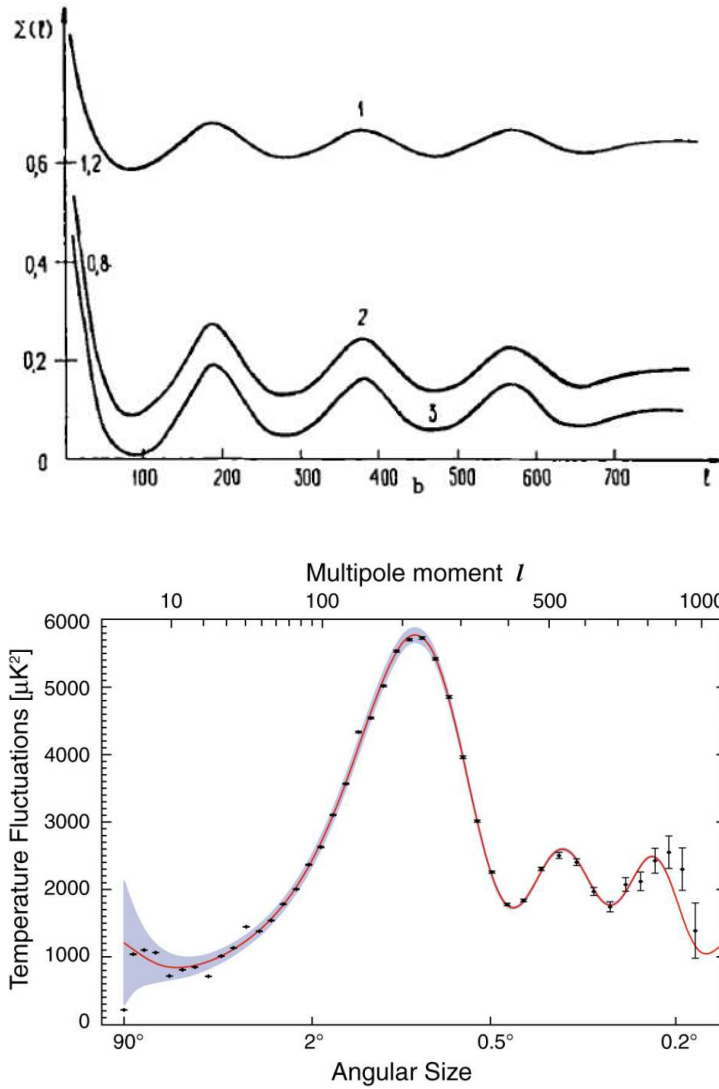


Figure 7: First prediction of the acoustic peaks in the spherical harmonics expansion of the CMB sky map (upper panel) and their modern version with observational data from the WMAP satellite (lower panel). Note that the position of the first peak was already similar to the observed one, although the normalization was completely different. The figure were taken from Zeldovich et al. (1972) and the WMAP web page <http://lambda.gsfc.nasa.gov/product/map/current/>.

pressure of the baryons and electrons $\sim 2N_b k T_\gamma$. As mentioned above, the specific entropy of our Universe is huge $N_\gamma/N_b \sim 10^9$, so that under these circumstances the *sound velocity* $v_s \sim c/\sqrt{3[1 + 3\epsilon_b/4\epsilon_r]}$ was close to speed of light and the *Jeans wavelength* was close to the horizon. According to the theory of Jeans instability adiabatic perturbations smaller than Jeans wavelength should evolve as *sound waves*. GR gives the same answer: the growing mode of perturbations is initiating standing acoustic waves with wavelengths depending on the characteristic scale of the perturbation.

These acoustic waves existed till the time of hydrogen recombination. After recombination radiation rapidly became free and uniform, Jeans wavelength, defined by thermal velocities of hydrogen atoms $v_s \sim \sqrt{2kT_\gamma/m_H}$, decreased many orders of magnitude and only baryons remembered the *phases* which standing acoustic waves had at the moment of recombination. After recombination density perturbations began to grow according to a power law and gave rise to the large scale structure of the Universe, which we observe today. Nevertheless, this characteristic quasi-periodical dependence of the amplitude of perturbations was conserved up to the phase of nonlinear of growth (see lower panel in Fig. 6). This prediction was made by RS & Zeldovich (1970a) and in completely independent way by Peebles & Yu (1970). Today we quote this behavior of initial density perturbations as *baryonic acoustic oscillations*. It is important to repeat that recombination played crucial role in their appearance.

Simultaneously it was recognized that interaction of CMB photons with moving electrons and baryon density perturbations must lead to a quasiperiodic dependence of the amplitude of CMB angular fluctuations on angular scale. It was painful for young postdoc (RS) when Zeldovich deleted the words about importance of observational search and added the last phrase into the abstract of the paper by RS & Zeldovich (1970a): "*A detailed investigation of the spectrum of fluctuations may, in principle, lead to an understanding of the nature of initial density perturbations since a distinct periodic dependence of the spectral density of perturbations on wavelength (mass) is peculiar to adiabatic perturbations. Practical observations are quite difficult due to the smallness of the effects and the presence of fluctuations connected with discrete sources of radio emission*". Fortunately Zeldovich told afterwards that physics is beautiful and it is worth to publish this paper. RS was guilty himself because he simultaneously was trying to estimate the angular fluctuations due to presence of radiosources Longair 1969.

A little later, Zeldovich, Rakhmatulina and RS (1972) found that a spherical harmonic expansion of the future CMB sky map should demonstrate the presence of CMB acoustic peaks (see upper panel in Fig. 7). Silk damping (Silk, 1968) was taken into account by Doroshkevich et al. (1978), who performed realistic computations of acoustic peaks in the baryon dominated Universe. When it was realized that our Universe contains cold dark matter, detailed analysis (Peebles, 1982; Bond & Efstathiou, 1984; Vittorio & Silk, 1984) showed that baryonic acoustic oscillations should remain important in the modern picture of the Universe. The predicted acoustic peaks on the CMB sky were observed in detail by Boomerang and MAXIMA1 balloon flights and WMAP spacecraft. Sloan Digital Sky Survey (Eisenstein et al., 2005; Hütsi, 2006) demonstrated the presence of baryonic oscillations in the spatial distribution of luminous red galaxies.

The visibility function and its importance

The Universe was optically thick before recombination, i.e. the mean free path of CMB photons was much smaller than the horizon. After recombination there were practically no free electrons left and the Universe became transparent; since then photons could propagate directly to us. Hydrogen recombination defines the *last scattering surface*.

The importance of the *Thomson visibility function* $V = \exp(-\tau_T) \times d\tau_T/dz$ was recognized already in RS and Zeldovich (1970), when an approximate analytical solution for recombination was found. This function defines the properties of the *last scattering surface*. We should mention here that these beautiful termini were introduced much later. We present the shape of the visibility function in Fig. 5.

The era of precision cosmology

The results from Boomerang, MAXIMA1 and WMAP together with supernovae Ia observations (Perlmutter et al., 1999; Riess et al., 1999) and the curve of growth for clusters of galaxies (see Vikhlinin et al., 2009, and references therein) opened the *era of precision cosmology*, providing detailed information about the key parameters of our Universe. It is obvious that the position and relative amplitude of acoustic peaks is defined by key parameters of the Universe and physical constants. At the same time the corresponding angular separation of acoustic peaks provides us with unique information about the distance to the *last scattering surface*. This demonstrates the great importance of the process of recombination. Any change in its position or in its sharpness will provide additional and crucial uncertainty in the determination of major parameters of the Universe. This is the reason why now we are trying to study the process of recombination with highest possible precision. It was a surprise for a majority of theorists that the expected precision of the Planck Surveyor spacecraft will be close to or significantly higher than the precision of widely used present day recombination codes.

2 The cosmological recombination radiation

2.1 Contributions due to standard hydrogen recombination

Within the picture described above it is possible to compute the *cosmological hydrogen recombination spectrum* with high accuracy. The photons corresponding to this spectral distortion of the CMB have been emitted mostly at redshifts $z \sim 1300 - 1400$, and therefore reach the observer today $\sim 10^3$ times redshifted. In Figure 8 we give the results of our computations for frequencies from 100 MHz up to 3000 GHz. The free-bound and bound-bound atomic *transitions among 5050 atomic levels* had to be taken into account in these computations. At high frequencies one can clearly see the features connected with the Lyman- α line, and the Balmer-, Paschen- and Brackett-series, whereas below $\nu \sim 1$ GHz the lines coming from transitions between highly excited level start to merge to a continuum. Also the features due to the Balmer and the 2s-1s two-photon continuum are visible. Overall the free-bound emission contributes

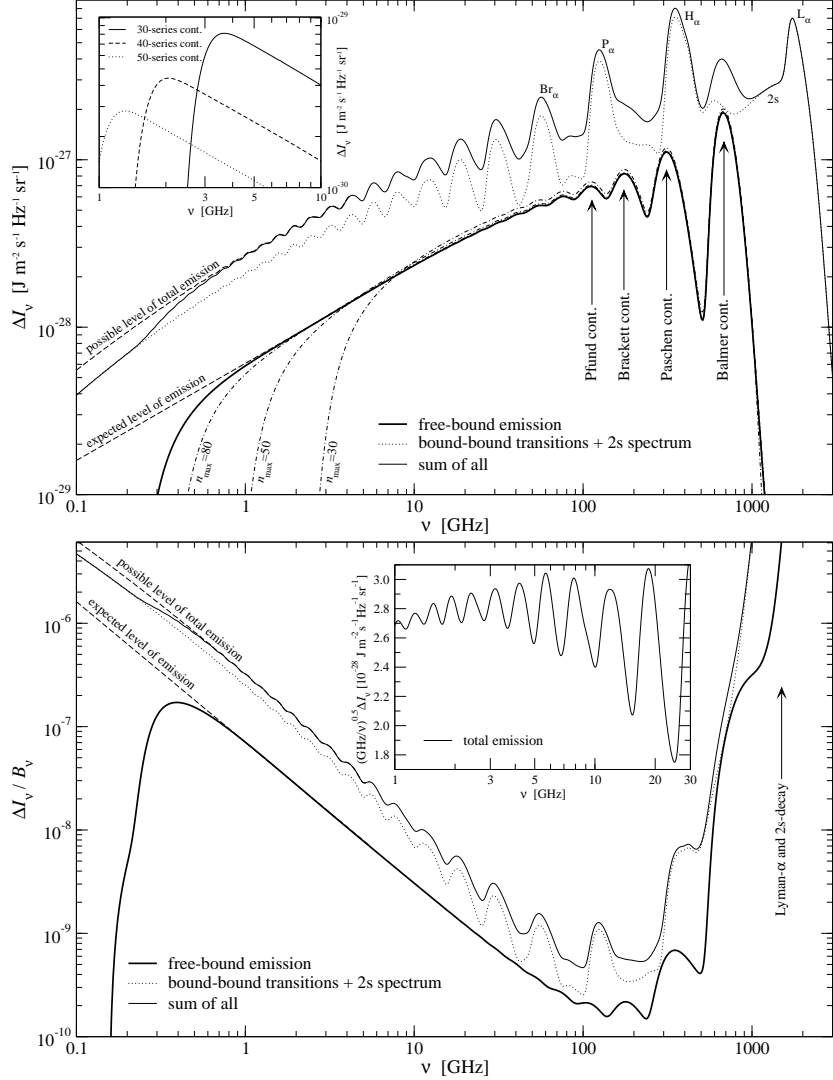


Figure 8: The full hydrogen recombination spectrum including the free-bound emission. The results of the computation for 100 shells were used. The contribution due to the 2s two-photon decay is also accounted for. The dashed lines indicate the expected level of emission when including more shells. In the upper panel we also show the free-bound continuum spectrum for different values of n_{\max} (dashed-dotted). The inlay gives the free-bound emission for $n = 30, 40,$ and 50 . The lower panel shows the distortion relative to the CMB blackbody spectrum, and the inlay illustrates the modulation of the total emission spectrum for $1 \text{ GHz} \leq \nu \leq 30 \text{ GHz}$ in convenient coordinates. The figure is from Chluba & RS (2006b).

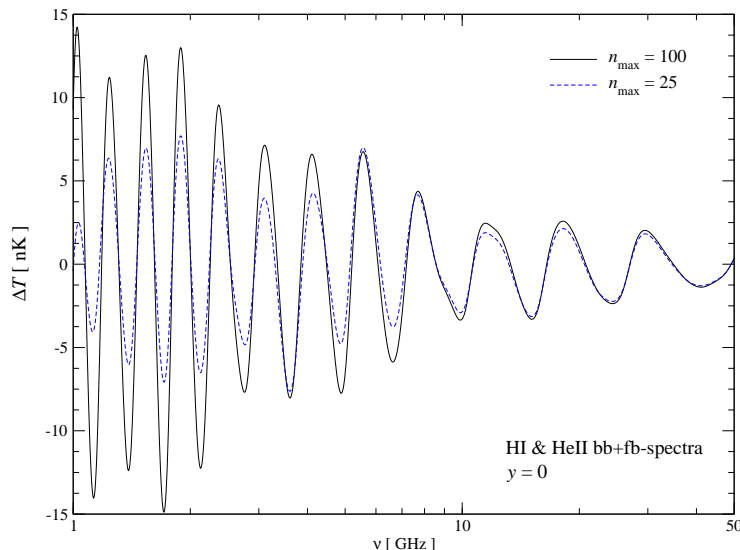


Figure 9: Frequency-dependent modulation of the CMB temperature caused by photons from the H I and He II recombination epochs. Both the bound-bound and free-bound contributions were included, and the mean recombination spectrum was subtracted. The shown signal is practically *unpolarized* and the same in *all* directions on the sky. The figure is taken from Chluba & RS (2009b).

about 20%-30% to the spectral distortion due to hydrogen recombination at each frequency, and a total of ~ 5 photons per hydrogen atom are released in the full hydrogen recombination spectrum.

One can also see from Figure 8 that both in the Wien and the Rayleigh-Jeans region of the CMB blackbody spectrum the relative distortion is growing. In the vicinity of the Lyman- α line the relative distortion exceeds unity by several orders of magnitude, but unfortunately at these frequencies the cosmic infra-red background due to sub-millimeter, dusty galaxies renders a direct measurement impossible. Similarly, around the maximum of the CMB blackbody at ~ 150 GHz it will likely be hard to measure these distortions with current technology, although there the spectral variability of the recombination radiation is largest. However, at low frequencies ($\nu \lesssim 2$ GHz) the relative distortion exceeds the level of $\Delta I/I \sim 10^{-7}$ but still has variability with well-defined frequency dependence at a level of several percent.

As additional example, the total recombination spectrum from hydrogen and He II at frequencies in the range $1 \text{ GHz} \lesssim \nu \lesssim 10 \text{ GHz}$ leads to a frequency-dependent modulation of the CMB temperature by $\Delta T \sim \pm 5 - 15 \text{ nK}$ (see Fig. 9 for more details), where the signal is expected to have many spectral features over one octave or one decade in frequency. These signatures from the cosmological recombination epochs are very hard to mimic by other astrophysical sources or instrumental noise, so that it may become possible to extract them in the future (see Sect. 2.4 for illustration of a possible observing strategy).

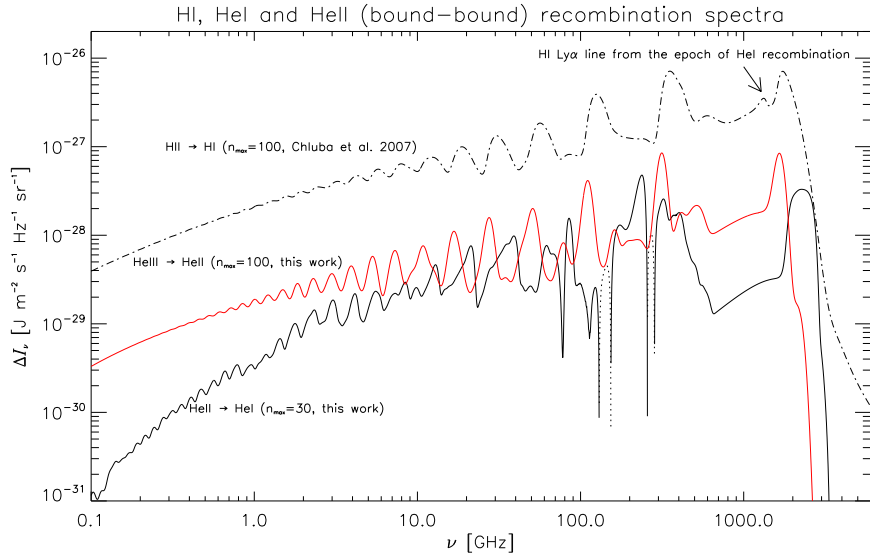


Figure 10: Helium and hydrogen (bound-bound) recombination spectra. The following cases are shown: (a) the $\text{He II} \rightarrow \text{He I}$ recombination spectrum (black solid line), which has been obtained including up to $n_{\text{max}} = 30$ shells, and considering all the J-resolved transitions up to $n = 10$. In this case, there are two negative features, which are shown (in absolute value) as dotted lines; (b) the $\text{He III} \rightarrow \text{He II}$ recombination spectrum (red solid line), where we include $n_{\text{max}} = 100$ shells, resolving all the angular momentum sub-levels and including the effect of Doppler broadening due to scattering off free electrons; (c) the H I recombination spectrum, where we plot the result from Chluba et al. (2007) up to $n_{\text{max}} = 100$. The H I Lyman- α line arising in the epoch of He I recombination is also added to the hydrogen spectrum (see the feature around $\nu = 1300$ GHz). In all three cases, the two-photon decay continuum of the $n = 2$ shell was also incorporated. The figure is taken from Rubiño-Martín et al. (2008).

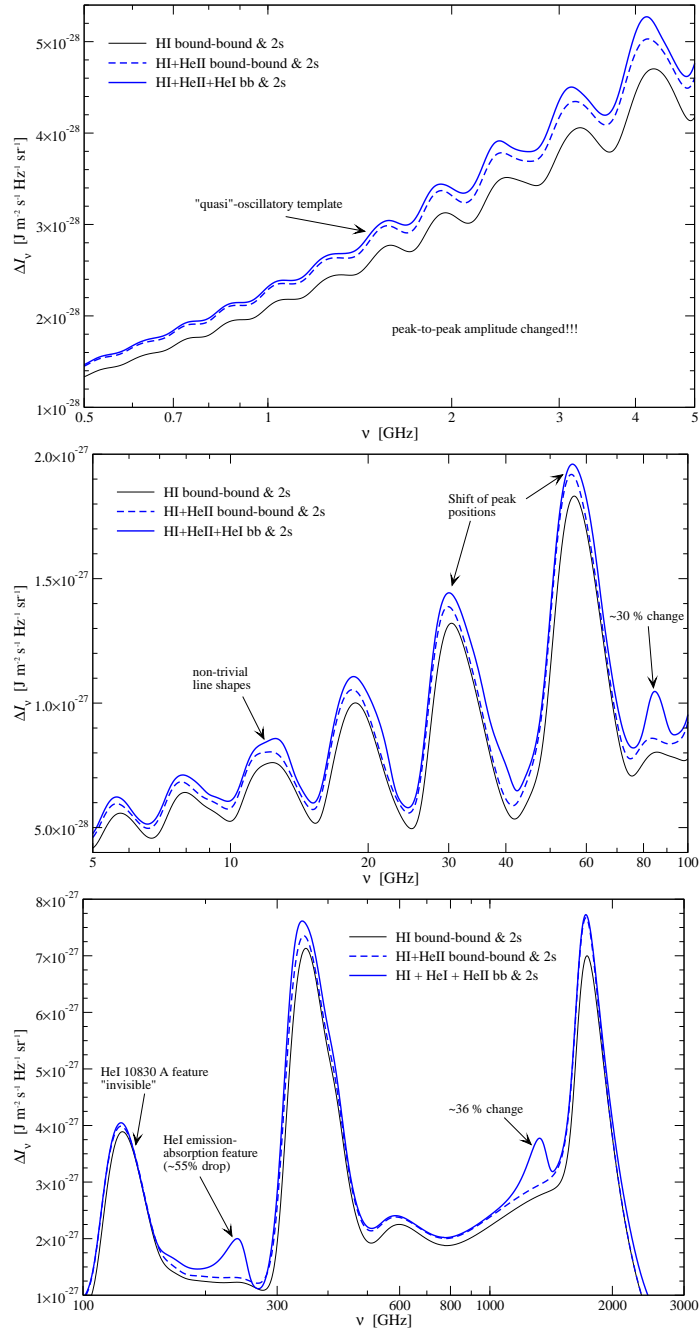


Figure 11: Helium and hydrogen (bound-bound) recombination spectra in different frequency bands. The curves were obtained summing the results shown in Fig. 10. In the figures we also pointed out some of the most significant additions to the pure hydrogen recombination spectrum, which are only because of the presence of pre-stellar helium in the primordial plasma.

2.2 The contributions due to standard helium recombination

Why would one expect any significant contribution to the cosmological recombination signal from helium, since it adds only $\sim 8\%$ to the total number of atomic nuclei? First of all, there are *two* epochs of helium recombination, i.e. $1600 \lesssim z \lesssim 3500$ for $\text{He II} \rightarrow \text{He I}$ and $5000 \lesssim z \lesssim 8000$ for $\text{He III} \rightarrow \text{He II}$ recombination. Therefore, overall one can already expect some $\sim 16\%$ contribution to the recombination spectrum due to the presence of helium in the Universe. However, it turns out that in some spectral bands the total emission due to helium transitions can reach amplitudes up to $\sim 30\% - 50\%$ (Rubiño-Martín et al., 2008). This is possible, since $\text{He III} \rightarrow \text{He II}$ actually occurs much faster, following the Saha-solution much closer than in the case of hydrogen recombination. Therefore photons are emitted in a narrower range of frequencies, and even the line broadening due to electron scattering cannot alter the shape of the features significantly until today (see Fig. 10).

In addition, the recombination of neutral helium is sped up due to the absorption of $2^1\text{P}_1 - 1^1\text{S}_0$ and $2^3\text{P}_1 - 1^1\text{S}_0$ -photons by the tiny fraction of neutral hydrogen already present at redshifts $z \lesssim 2400$. This process was suggested by P. J. E. Peebles in the mid 90's (see remark in Hu et al., 1995), but only recently it has been convincingly taken into account by Switzer & Hirata (2008a) and others (Kholupenko et al., 2007; Rubiño-Martín et al., 2008). This also makes the neutral helium lines more narrow and enhances the emission in some frequency bands (see Fig. 10 and for more details Fig. 11). Also the re-processing of helium photons by hydrogen lead to additional signatures in the recombination spectrum, most prominently the 'pre-recombinational' H I Lyman- α line close to $\nu \sim 1300$ GHz (see Fig. 11).

We would like to mention, that the first computations of the helium recombination spectrum were performed by Dubrovich & Stolyarov (1997), before the cosmological concordance model was actually established. Also neutral helium recombination was still considered to occurs much slower, since the effect connected to the hydrogen continuum opacity was not taken into account, and the existing atomic data for He I was still rather poor. In the most recent computations of the neutral helium spectrum (Rubiño-Martín et al., 2008), for both the singlet and triplet atom, up to $n_{\text{max}} = 30$ shells were included. This amounts in a total of ~ 1000 different atomic levels. Furthermore, we have taken into account all fine-structure and most of the singlet-triplet transitions for levels with $n \leq 10$, using the atomic data published by Drake & Morton (2007) and according to the approach discussed with Beigman & Vainshtein (2009). In the case of neutral helium, the non-trivial superposition of all lines even lead to the appearance of two *negative features* in the total He I bound-bound recombination spectrum (see Fig. 10). The one at $\nu \sim 145$ GHz is coming from one of the 10830 Å fine-structure lines, whereas the feature close to $\nu \sim 270$ GHz is mainly due to the superposition of the negative 5877 Å and positive 6680 Å-lines (Rubiño-Martín et al., 2008).

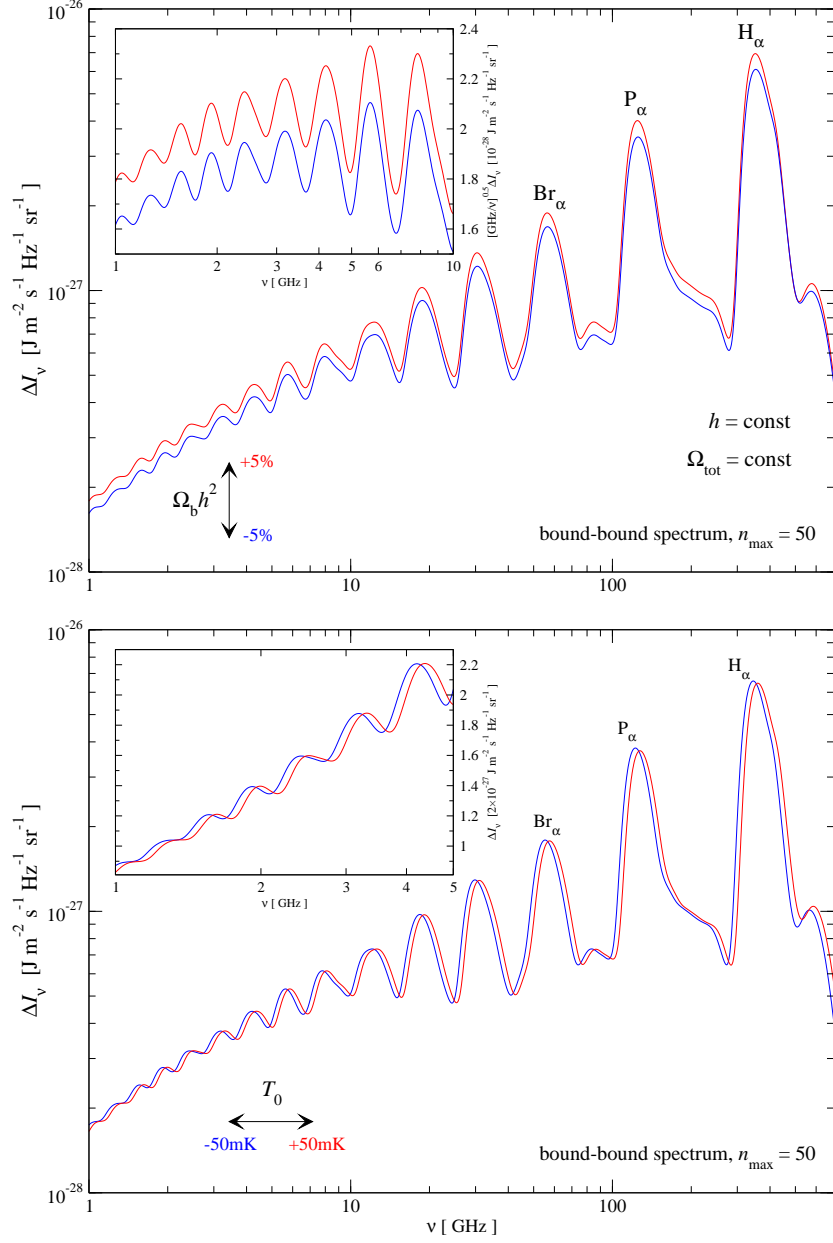


Figure 12: The bound-bound hydrogen recombination spectrum for $n_{\max} = 50$. The upper panel illustrates the dependence on $\Omega_b h^2$, and the lower the dependence on the value of T_0 . The figure is from Chluba & RS (2008a).

2.3 Dependence of the recombination spectrum on cosmological parameters

In this Section we want to *illustrate* the impact of different cosmological parameters on the hydrogen recombination spectrum. We restricted ourselves to the bound-bound emission spectrum and included 50 shells for the hydrogen atom into our computations.

In Fig. 12 we illustrate the dependence of the hydrogen recombination spectrum on the value of the CMB monopole temperature, T_0 . The value of T_0 mainly defines the time of recombination, and consequently when most of the emission in each transition appears. This leads to a dependence of the *line positions* on T_0 , but the total intensity in each transition (especially at frequencies $\nu \lesssim 30$ GHz) remains practically the same. We found that the fractional shift of the low frequency spectral features along the frequency axis scales roughly like $\Delta\nu/\nu \sim \Delta T/T_0$. Hence $\Delta T \sim 1$ mK implies $\Delta\nu/\nu \sim 0.04\%$ or $\Delta\nu \sim 1$ MHz at 2 GHz, which with modern spectrometers is rather easy to resolve. Since the maxima and minima of the line features due to the large duration of recombination are rather broad ($\sim 10\% - 20\%$), it is probably better to look for these shifts close to the steep parts of the lines, where the derivatives of the spectral distortion due to hydrogen recombination are largest. It is also important to mention that the hydrogen recombination spectrum is shifted as a *whole*, allowing to increase the significance of a measurement by considering many spectral features at several frequencies.

We showed in Chluba & RS (2008a) that the cosmological hydrogen recombination spectrum is practically independent of the value of h . Only the features due to the Lyman, Balmer, Paschen and Brackett series are slightly modified. This is connected to the fact, that h affects the ratio of the atomic time-scales to the expansion time. Therefore changing h affects the escape rate of photons in the Lyman- α transition and the relative importance of the 2s-1s transition. For transitions among highly excited states it is not crucial via which channel the electrons finally reach the ground state of hydrogen and hence the modifications of the recombination spectrum at low frequencies due to changes of h are small. Changes of $\Omega_m h^2$ should affect the recombination spectrum for the same reason.

The lower panel in Fig. 12 illustrates the dependence of the hydrogen recombination spectrum on $\Omega_b h^2$. It was shown that the total number of photons released during hydrogen recombination is directly related to the total number of hydrogen nuclei (e.g. Chluba & RS, 2008a). Therefore one expects that the overall *normalization* of the recombination spectrum depends on the total number of baryons, $N_b \propto \Omega_b h^2$, and the helium to hydrogen abundance ratio, Y_p . Varying $\Omega_b h^2$ indeed leads to a change in the overall amplitude $\propto \Delta(\Omega_b h^2)/(\Omega_b h^2)$. Similarly, changes of Y_p should affect the normalization of the hydrogen recombination spectrum, but here it is important to also take the helium recombination spectrum into account. Like in the case of hydrogen there is an effective number of photons that is produced per helium atom during $\text{He III} \rightarrow \text{He II}$ and $\text{He II} \rightarrow \text{He I}$ recombination. Changing Y_p will affect the relative contribution of hydrogen and helium to the cosmological recombination spectrum. Since the physics of helium recombination is different than in the case of hydrogen (e.g. the spectrum of neutral helium is more complicated; helium recombination occurs at earlier times, when the medium was hotter; $\text{He III} \rightarrow \text{He II}$ is more rapid, so that the recombination lines

are more narrow), one can expect to find direct evidence of the presence of helium in the full recombination spectrum. These might be used to quantify the total amount of helium during the epoch of recombination, well before the first appearance of stars.

2.4 A possible observing strategy

In order to measure the distortions under discussion one should scan the CMB spectrum along the *frequency axis* including several spectral bands (for illustration see Fig. 13). Because the CMB spectrum is the *same in all directions*, one can collect the flux of large regions on the sky, particularly choosing patches that are the least contaminated by other astrophysical foregrounds. Also the recombinational signals should be practically *unpolarized*, a fact that provides another way to distinguish it from other possible contaminants. *No absolute measurement* is necessary, but one only has to look for a modulated signal at the $\sim \mu\text{K}$ level, with typical peak-to-peak amplitude of $\sim 10\text{--}30\text{ nK}$ and $\Delta\nu/\nu \sim 0.1$ (e.g. see Fig. 9), where this signal can be predicted with high accuracy, yielding a *spectral template* for the full cosmological recombination spectrum, which should also include the contributions from helium. Note that for observations of the CMB temperature anisotropies a sensitivity level of 10 nK in principle can be already achieved (Readhead, 2007).

We want to stress again, that measuring these distortions of the CMB spectrum would provide a way to confront our understanding of the recombination epoch with *direct experimental evidence*, and in principle may deliver another independent method to determine some of the key parameters of the Universe, in particular the value of the CMB monopole temperature, T_0 , the number density of baryons, $\propto \Omega_b h^2$, and the pre-stellar helium abundance, *not suffering* from limitations set by *cosmic variance* (see Sect. 2.3 for more details). As we will explain in the next section, most importantly if something *non-standard* occurred during or before the epoch of cosmological recombination, this should leave some potentially observable traces in the cosmological recombination radiation, which would allow us to learn additional details about the *thermal history* of our Universe.

2.5 The cosmological recombination radiation after energy release before the end of hydrogen recombination

All the computations for the standard cosmological recombination spectrum presented in the previous sections were performed assuming that at all times the ambient CMB radiation field is given by a *pure blackbody* spectrum with temperature $T_\gamma \propto (1+z)$. Furthermore, it is assumed that the distortions created in the recombination epochs are negligibly small, except for those from the main resonances, e.g. the Lyman series in the case of hydrogen. These assumptions are very well justified for a *standard thermal history* of the Universe, since the expansion of the Universe alone does not alter the shape of the photon distribution. Therefore it is clear that well *before* the recombination epoch atomic emission and absorption processes are balancing each other with extremely high precision, so that no net signal to the CMB spectrum can be created.

However, it is well known that the CMB spectrum in principle could deviate from a pure blackbody, if at some point some *energy release* (e.g. due to decaying or anni-

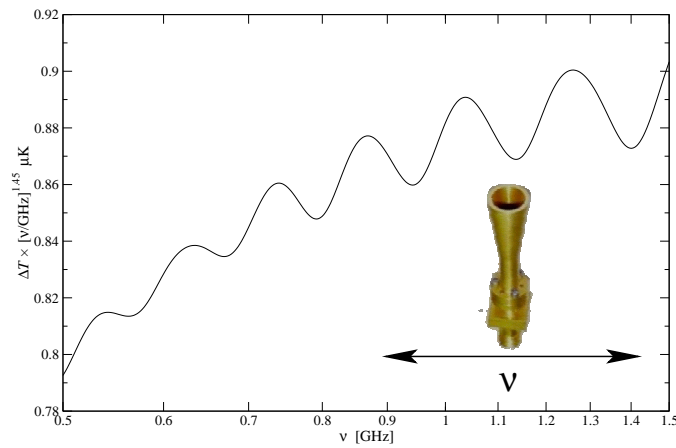
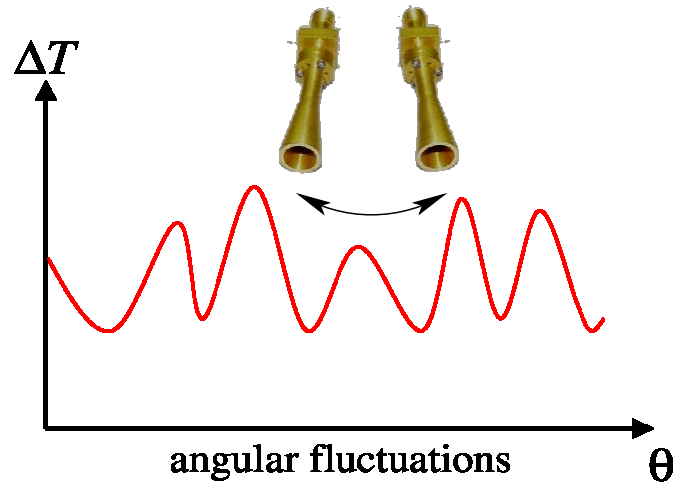


Figure 13: Comparison of observing strategies: top panel – observations of the CMB temperature anisotropies. Here one is scanning the sky at fixed frequency in different directions. lower panel – proposed strategy for the signal from cosmological recombination. For this one may fix the observing direction, choosing a large, least contaminated part of the sky, and scan along the frequency axis instead.

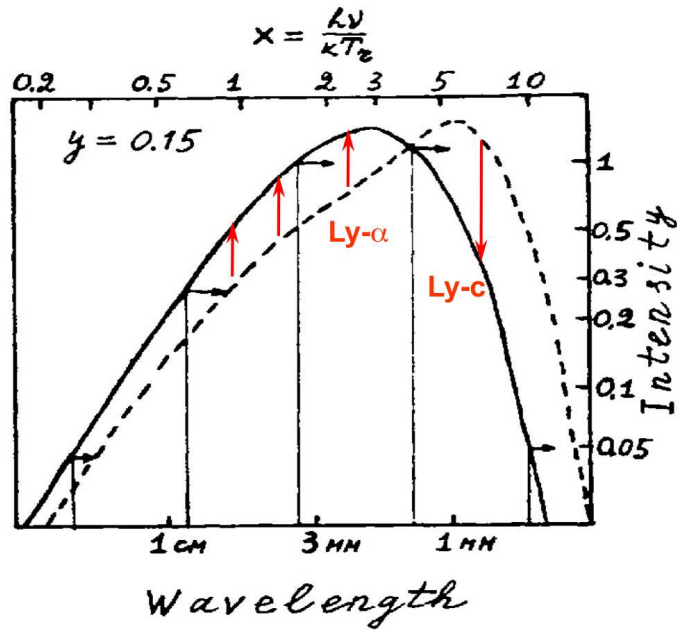


Figure 14: Illustration of a Compton y -distortion for $y = 0.15$. The solid line shows that CMB blackbody spectrum, while the dashed line represents the distorted CMB spectrum. The figure was adapted from RS & Zeldovich (1980).

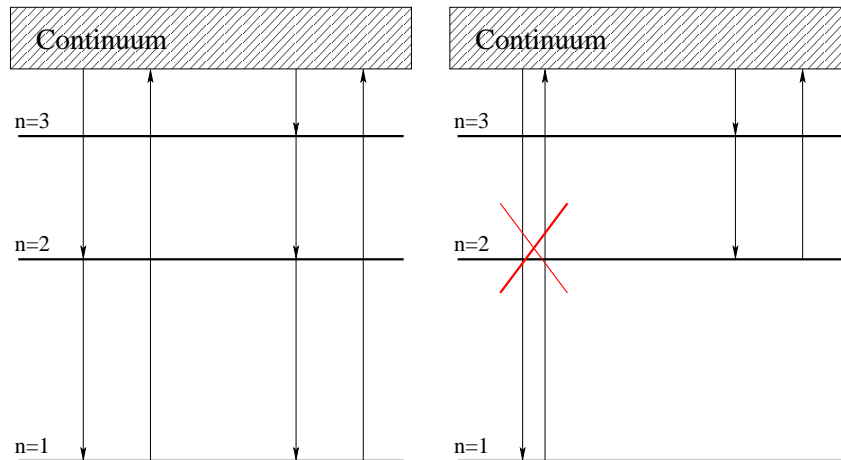


Figure 15: Sketch of the main atomic loops for hydrogen and He II when including 3 shells. The left panel shows the loops for transitions that are terminating in the Lyman-continuum. The right panel shows the case, when the Lyman-continuum is completely blocked, and unbalanced transitions are terminating in the Balmer-continuum instead. In the first case up to 3 photons can be created per absorbed Lyman continuum photon, while in the later 2 photons are released per absorbed Balmer continuum photon. The figure was taken from Chluba & RS (2009b)

hilating particles) occurred, leading to a *non-standard thermal history* of the Universe. For early energy release ($5 \times 10^4 \lesssim z \lesssim 2 \times 10^6$) the resulting spectral distortion can be characterized as a Bose-Einstein μ -type distortion (RS & Zeldovich, 1970b; Illarionov & RS, 1975a,b), while for energy release at low redshifts ($z \lesssim 5 \times 10^4$) the distortion is close to a y -type distortion (Zeldovich & RS, 1969). The current best observational limits on these types of distortions were obtained using the COBE/FIRAS instrument, yielding $|y| \leq 1.5 \times 10^{-5}$ and $|\mu| \leq 9.0 \times 10^{-5}$ (Fixsen et al., 1996). Here we now want to address the question of how a y -distortion with $y \lesssim 1.5 \times 10^{-5}$ would affect the cosmological recombination radiation and what one could learn about the mechanism that lead to the energy injection by observing the recombinational radiation.

Transition loops in a non-blackbody ambient radiation field

If we assume that at redshift $z_i \lesssim 5 \times 10^4$ some amount of energy was released, then afterwards the intrinsic CMB spectrum deviates from a pure blackbody, where the spectral distortion will be given by a y -type distortion. The y -parameter will be directly related to the total amount of energy that was released, but here it only matters that it does not exceed the upper limit given by COBE/FIRAS. In comparison to the blackbody spectrum a y -type distortion¹ is characterized by a *deficit* of photons at low and an *increment* at high frequencies (see Fig. 14 for illustration).

It is clear that *after* the energy release the equilibrium between the matter and radiation is perturbed, and a small imbalance between atomic emission and absorption is created, which leads to the development of closed *loops* of transitions (Lyubarsky & RS, 1983). These loops can now produce a *net change* in the number of photons, even *prior* to the epoch of recombination, but otherwise they leave the ionization degree of the Universe unaltered. Also, it is expected that they should always form in such a way that the net destruction and creation of photons will tend to re-establish the full equilibrium between matter and radiation. As an example, if we consider a redshift at which the Lyman continuum frequency of hydrogen is located in the Wien part of the distorted CMB, while the other transitions are still in the Rayleigh-Jeans part of the spectrum (see Fig. 14 for illustration), then the excess of Lyman continuum photons over the value for the blackbody, will lead to an excess photo-ionization of hydrogen atoms from the ground-state. On the other hand, the deficit of photons in the low frequency part of the background radiation spectrum will allow slightly more electrons to be captured to (highly) excited states than for a blackbody ambient radiation field. From these excited states the electrons then can cascade down towards the ground state, emitting several low frequency photons during the dipole transition via intermediate levels. In this closed loop which started with the destruction of a Lyman-continuum photon, several low frequency photons can be created (see Fig. 15).

¹ This type of CMB distortion is also well known in connection with the thermal SZ-effect caused by the scattering of CMB photons by the hot electron plasma inside the deep potential wells of clusters of galaxies (RS & Zeldovich, 1980).

What one could learn from the pre-recombinational recombination radiation

The described process is expected to alter the total radiation coming from atomic transitions in the early Universe and may leave some observable spectral features in addition to those produced during the normal recombination epoch (see next section for details). The interesting point is that the photons which are created in these loops are emitted in the *pre-recombinational epoch* of the considered atomic species. Therefore, it will make a difference, if energy injection occurred *before* $\text{He III} \rightarrow \text{He II}$ recombination, at different stages *between* the three recombination epochs, or *after* hydrogen recombination finished (see Fig. 5 for reminder on the different recombination epochs). In particular, if energy injection occurred after hydrogen recombination finished, then there should be *no additional* traces of this energy injection in the recombinational radiation. This fact provides the interesting possibility to distinguish a pre-recombinational all sky y -distortion from the one that is created e.g. due to unresolved SZ-clusters, supernova explosions, or the warm-hot-intergalactic medium at redshift well below the recombination epoch. Here it is important that a normal y -distortion is *completely featureless*, so that it is very hard to tell when the distortion was introduced. However, the changes in the cosmological recombination radiation generated by energy injection before the end of hydrogen recombination not only depend on the *amount of energy* that was injected but also on the *time* and *duration* of this process (Chluba & RS, 2009b). Furthermore, energy injection does leave *distinct spectral features* in the recombinational radiation (see next section), which may allow us to learn much more than just confirming that there was some energy injection at some point.

Dependence of the cosmological recombination radiation on the y -parameter

Similar to the standard recombination spectrum it is possible to compute the recombination radiation assuming that the ambient CMB radiation field is given by a distorted blackbody, where the distortion is given by a y -distortion. We first want to address the question how the expected changes in the cosmological recombination radiation depend on the value of the y -parameter. Here the interesting question is if it will be possible to determine the value of the y -parameter using the frequency dependence of the CMB spectral distortion.

In Fig. 16 we show the results of these computations (Chluba & RS, 2009b). In each panel the blue solid line represents the contributions to the normal cosmological recombination spectrum (i.e. $y = 0$). For this case, one can see that the contribution from He II is about one order of magnitude smaller than the one from hydrogen. If we now allow a y distortion with $y = 10^{-7}$, then one can see that the contribution from hydrogen has not changed very much. Only a small negative feature, which was completely absent for $y = 0$, appeared at $\nu \sim 1200 - 1300$ GHz. It is mainly due to high redshift absorption in the Lyman-continuum and the Lyman-series with $n > 2$ (Chluba & RS, 2009b), and is also visible in the distortion caused by He II . One can also see that already for $y = 10^{-7}$ the contribution from He II changed more strongly than the one from hydrogen.

This becomes even more apparent, when further increasing the value of the y -parameter. Then for both helium and hydrogen the amplitude of the distortion changes

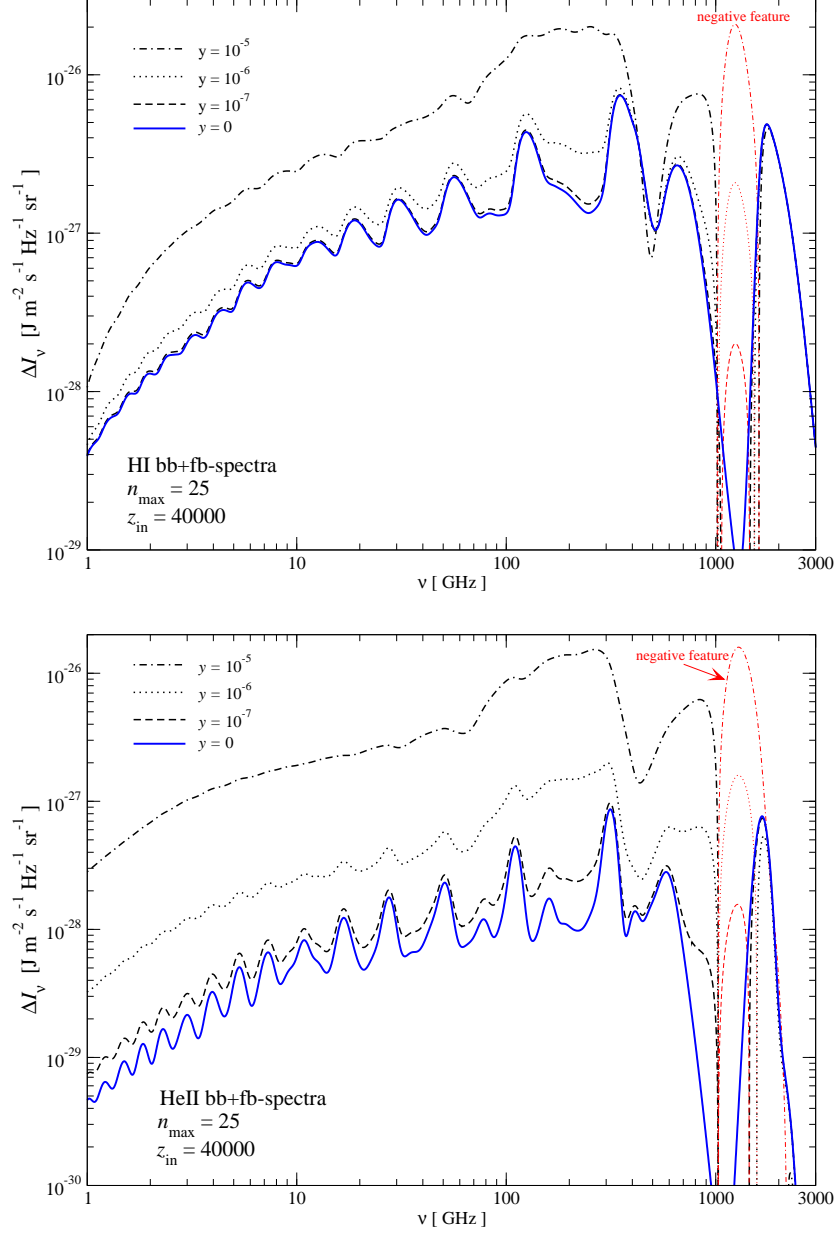


Figure 16: Contributions from the H I (upper panel) and He II (lower panel) to the total recombination spectrum for different values of the initial y -parameter. Both the bound-bound and free-bound signals were included. Energy injection was assumed to occur at $z_i = 4 \times 10^4$. The thin red lines represent the overall negative parts of the signals. We included 25 shells for both H I and He II into our computations. The figures were taken from Chluba & RS (2009b).

several times, where in particular the contribution from He II has become comparable to the one from hydrogen. This is due to the fact that the loops in helium can be run through ~ 8 times faster than hydrogen, because of the charge scaling of the atomic transition rates (see Chluba & RS, 2009b, for more detailed explanation). Also the negative feature became much more strong, in amplitude even exceeding the Lyman- α distortions from the main recombination epoch. At low frequencies not only the amplitude of the signal has increased, but also its frequency dependence has changed significantly. This may allow to determine the value of the y -parameter by measuring the frequency-dependent modulation of the CMB spectrum caused due to the presence of atomic species in the early Universe.

Similarly, one can ask how the changes in the cosmological recombination radiation depend on the time of the energy injection. The results of these computations are shown in Fig. 17. One can see that not only the overall amplitude of the distortion strongly depends on the time of energy injection, but also the shape and number of features changes drastically. This fact may allow us to understand when the y -distortion was actually introduced, and as explained above, at the very least should allow to distinguish *pre-* from *post-recombinational* y -distortions.

3 Previously neglected physical processes during hydrogen recombination

With the improvement of available CMB data also refinements of the computations regarding the ionization history became necessary, leading to the development of the widely used RECFast code (Seager et al., 1999, 2000; Wong et al., 2008). However, the prospects with the PLANCK Surveyor have motivated several groups to re-examine the problem of cosmological hydrogen and helium recombination, with the aim to identify previously neglected physical processes that could affect the ionization history of the Universe at the level of $\gtrsim 0.1\%$. Such accuracy becomes necessary to achieve the promised precision for the estimation of cosmological parameters using the observation of the CMB temperature anisotropies and acoustic peaks.

Here we wish to provide an overview of the most important additions in this context and to highlight some of the previously neglected physical processes during hydrogen recombination. Most of them are also important during the epoch of helium recombination (e.g. Switzer & Hirata, 2008a,b; Rubiño-Martín et al., 2008), but here we focus our discussion on hydrogen only. The superposition of all effects listed below lead to an ambiguity in the ionization history during the cosmological hydrogen recombination epoch that clearly exceeds the level of 0.1%, even reaching $\sim 1\% - 2\%$ close to the maximum of the Thomson visibility function, where it matters most. All these corrections therefore should be taken into account in the detailed analysis of future CMB data (for additional overview also see Fendt et al., 2009). Still the analysis shows that the simple picture, as explained in Sect. 1 is amazingly stable.

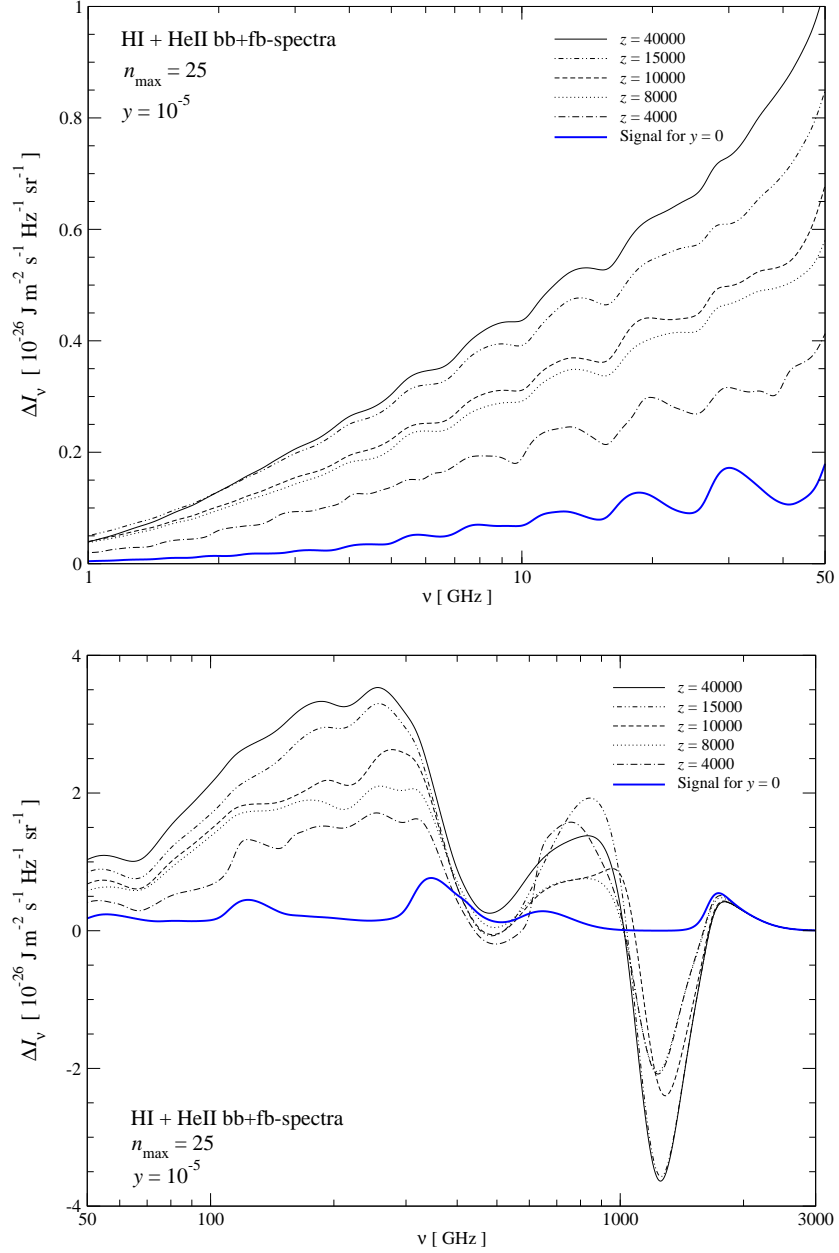


Figure 17: Total H I + He II recombination spectra for different energy injection redshifts. The upper panel shows details of the spectrum at low, the lower at high frequencies. We included 25 shells for both H I and He II into our computations. The figures were taken from Chluba & RS (2009b).

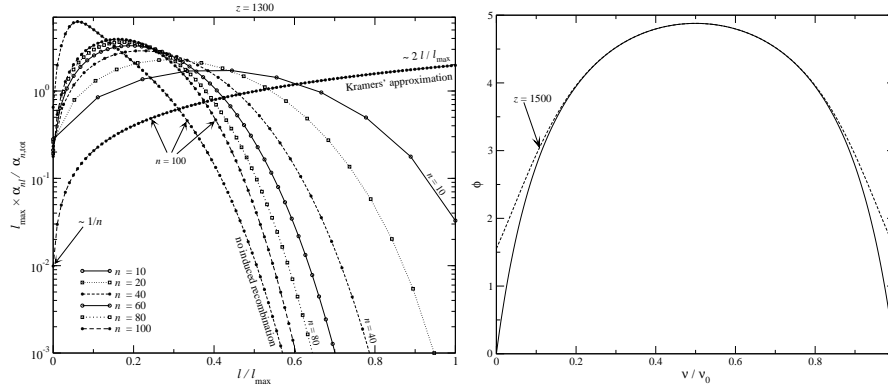


Figure 18: *Left panel* – l -dependence of the recombination coefficient, α_{nl} , at $z = 1300$ for different shells. The curves have been re-scaled by the *total* recombination coefficient, $\alpha_{n,\text{tot}} = \sum_l \alpha_{nl}$, and multiplied by $l_{\text{max}} = n - 1$ such that the 'integral' over $\xi = l/l_{\text{max}}$ becomes unity. Also the results obtained within the Kramer's approximation, i.e. $\alpha_{nl}^{\text{K}} = \text{const} \times [2l + 1]$, and without the inclusion of stimulated recombination for $n = 100$ are presented. *Right panel* – Two-photon decay profile for the 2s-level in hydrogen: the solid line shows the broad two-photon continuum assuming that there is no ambient radiation field. In contrast, the dashed line includes the effects of induced emission due to the presence of CMB photons at $z = 1500$. The figures are from Chluba & RS (2006a) and Chluba et al. (2007).

Detailed evolution of the populations in the angular momentum sub-states

The numerical solution of the hydrogen recombination history and the associated spectral distortions of the CMB requires the integration of a stiff system of coupled ordinary differential equations, describing the evolution of the populations of the different hydrogen levels, with extremely high accuracy. Until recently this task was only completed using additional simplifying assumptions. Among these the most important simplification is to assume *full statistical equilibrium*² (SE) within a given shell for $n > 2$. (for a more detailed comparison of the different approaches see Rubiño-Martín et al. (2006) and references therein). However, as was shown in Rubiño-Martín et al. (2006) and Chluba et al. (2007), this leads to an overestimation of the hydrogen recombination rate at low redshift by up to $\sim 3\% - 5\%$. This is mainly because during hydrogen recombination collisions are so much weaker than radiative processes, so that the populations within a given atomic shell depart from SE. It was also shown that for the highly excited levels stimulated emission and recombination (see Fig. 18) are important.

Induced two-photon decay of the hydrogen 2s-level

In the transition of electrons from the 2s-level to the ground state two photons are emitted in a broad continuum (see Fig. 18). Due to the presence of a large number of CMB photons at low frequencies, stimulated two-photon emission becomes important

²i.e. the population of a given level (n, l) is determined by $N_{nl} = (2l + 1)N_n/n^2$, where N_n is the total population of the shell with principle quantum number n .

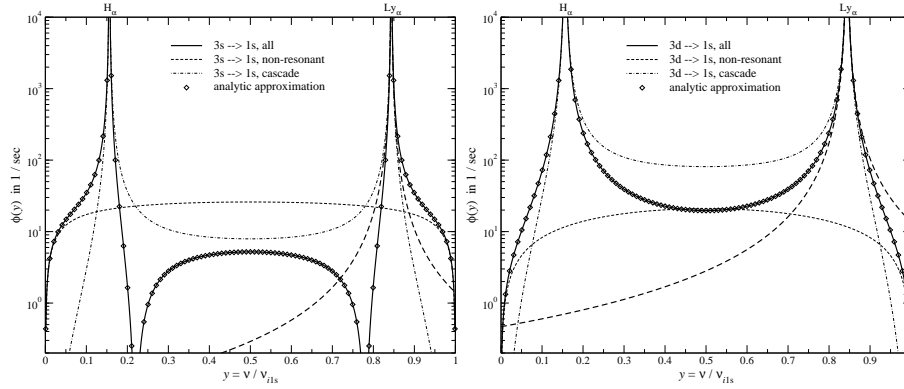


Figure 19: Two-photon emission profile for the $3s \rightarrow 1s$ and $3d \rightarrow 1s$ transition. The non-resonant, cascade and combined spectra are shown as labeled. Also we give the analytic approximation as given in Chluba & RS (2008b) and show the usual Lorentzian corresponding to the Lyman- α line (long dashed). The figure is from Chluba & RS (2008b).

when one of the photons is emitted close to the Lyman- α transition frequency, and, as demonstrated in Chluba & RS (2006a), leads to an increase in the effective $2s$ - $1s$ two-photon transition rate during hydrogen recombination by more than 1%. This speeds up the rate of hydrogen recombination, leading to a maximal change in the ionization history of $\Delta N_e/N_e \sim -1.3\%$ at $z \sim 1050$.

Re-absorption of Lyman- α photons

The strongest distortion of the CMB blackbody spectrum is associated with the Lyman- α transition and $2s$ - $1s$ continuum emission. Due to redshifting these excess photons can affect energetically lower transitions. The huge excess of photons in the Wien-tail of the CMB slightly increases the $1s \rightarrow 2s$ two-photon absorption rate, resulting in percent-level corrections to the ionization history during hydrogen recombination with $\Delta N_e/N_e \sim +1.9\%$ at $z \sim 1020$ (Kholupenko & Ivanchik, 2006).

Feedback within the H I Lyman-series

Due to redshifting, all the Lyman-series photons emitted in the transition of electrons from levels with $n > 2$ have to pass through the next lower-lying Lyman-transition, leading to additional feedback corrections like in the case of Lyman- α absorption in the $2s$ - $1s$ two-photon continuum. However, here the photons connected with Ly_n are completely absorbed by the $Ly(n-1)$ resonance and eventually all Ly_n photons are converted into Lyman- α or $2s$ - $1s$ two-photon decay quanta. Also in the computations one has to take into account that the feedback of Ly_n photons on the $Ly(n-1)$ resonance occurs some time after the photon was released. For example for $Ly\beta$ to $Ly\alpha$ the feedback happens $\Delta z/z \sim 16\%$ after the emission. As shown by Chluba & RS (2007), feedback of photons within the H I Lyman-series leads to a correction in the ionization history of $\Delta N_e/N_e \sim 0.2\% - 0.3\%$ at $z \sim 1050$.

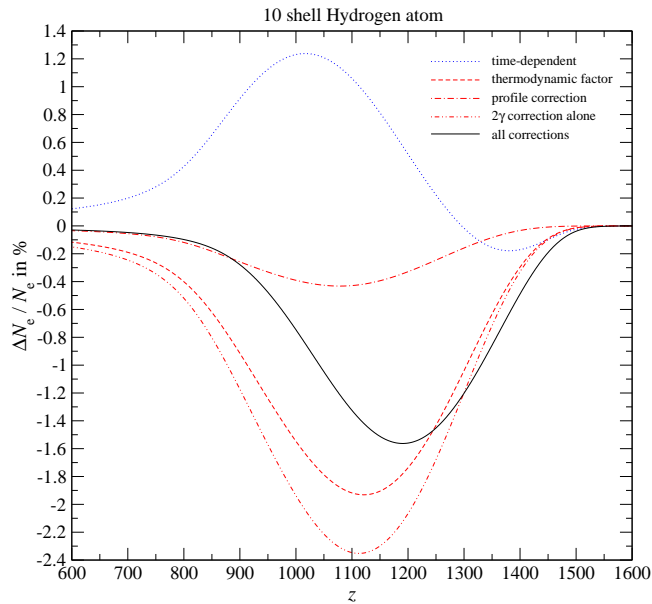


Figure 20: Changes in the free electron fraction: separate contributions due to the *time-dependent* correction, the *thermodynamic factor* and the *shape* of the profile. The figure was taken from Chluba & RS (2009c).

Two-photon transitions from higher levels

One of the most promising additional corrections to the ionization history is due to the two-photon transition of highly excited hydrogen states to the ground state as proposed by Dubrovich & Grachev (2005). The estimated correction was anticipated to be as large as $\sim 5\%$ very close to the maximum of the Thomson visibility function, and therefore should have had a large impact on the theoretical predictions for the CMB power spectra. It is true that in the extremely low density plasmas the cascade of permitted transitions (for example the chain $3s \rightarrow 2p \rightarrow 1s$) goes unperturbed and might be considered as two photon process with two resonances (Göppert-Mayer, 1931). In addition there is a continuum, analogues to $2s-1s$ decay spectrum, and an interference term between resonant contributions and this weak continuum (see Fig. 19 and Chluba & RS (2008b)). However, the estimates of Dubrovich & Grachev (2005) only included the contribution to the two-photon decay rate coming from the two-photon continuum, which is due to virtual transitions, and as for example shown in Chluba & RS (2008b) in particular the interference between resonant and non-resonant contributions plays an important role in addition. This results in deviations of the line emission profiles from the normal Lorentzian shape, which are caused by quantum mechanical aspects of the problem and are most strong in the distant damping wings (e.g. see Fig. 19).

Furthermore, as for example pointed out by Chluba & RS (2008b) the full problem has to include aspects of the radiative transfer in the main resonances, since some significant fraction of photons are also escaping from within a few ten to hundred

Doppler width of the line centers. In addition, at the percent-level even in the very distant damping wings (i.e. $10^2 - 10^3$ Doppler width away from the line center) radiative transfer is still important, leading to additional re-absorption of photons before they finally escape. Recently this problem was considered in detail by Chluba & RS (2009c) for the 3d-1s and 3s-1s two-photon transitions. In their analysis, three independent sources of corrections were identified (we will discuss the other two processes below), showing that the total modification coming from purely quantum mechanical aspects of the problem lead to a change in the free electron number of $\Delta N_e/N_e \sim -0.4\%$ at $z \sim 1100$ (see Fig. 20 for more detail).

Time-dependent aspects in the emission and absorption of Lyman α photon

One of the key ingredients for the derivation of the escape probability in the Lyman α resonance using the Sobolev approximation (Sobolev, 1960) is the *quasi-stationarity* of the line transfer problem. However, as shown recently (Chluba & RS, 2009a,c) at the percent-level this assumption is not justified during the recombination of hydrogen, since (i) the ionization degree, expansion rate of the Universe and Lyman α death probability change over a characteristic time $\Delta z/z \sim 10\%$, and (ii) because a significant contribution to the total escape probability is coming from photons emitted in the distant wings (comparable to $10^2 - 10^3$ Doppler width) of the Lyman α resonance. Therefore one has to include *time-dependent aspects* in the emission and absorption process into the line transfer problem, leading to a delay of recombination by $\Delta N_e/N_e \sim +1.2\%$ at $z \sim 1000$ (see Fig. 20 for more detail).

Thermodynamic asymmetry in the Lyman α emission and absorption profile

Knowing the shape of the Lyman α line emission profile³ and applying the *detailed balance principle*, one can directly obtain an expression for the line absorption profile. With this one finds that there is a *frequency-dependent asymmetry* between the line emission and absorption profile, which becomes strongest at large distances (beyond $10^2 - 10^3$ Doppler width) from the line center. This asymmetry is given by a *thermodynamic correction factor* (Chluba & RS, 2009c), which has an exponential dependence on the *detuning* from the line center, i.e. $f_\nu \propto \exp(h[\nu - \nu_\alpha]/kT_\gamma)$, where ν_α is the transition frequency for the Lyman alpha resonance. Usually this factor can be neglected, since for most astrophysical problems the main contribution to the number of photons is coming from within a few Doppler width of the line center, where the thermodynamic factor indeed is very close to unity. However, as mentioned above, in the Lyman α escape problem during hydrogen recombination also contributions from the very distant damping wings are important, so that there $f_\nu \neq 1$ has to be included.

In the normal '1 + 1' photon picture for the line emission and absorption process f_ν has no direct physical interpretation. It is simply the result of thermodynamic requirements necessary to preserve a blackbody spectrum at all frequencies from the line center in the case of full thermodynamic equilibrium. However, as explained by Chluba & RS (2009c), in the two photon picture f_ν is due to the fact that in the recombination problem the photon distribution for transitions from the 2p-state towards higher

³It is usually assumed to be given by a Voigt profile.

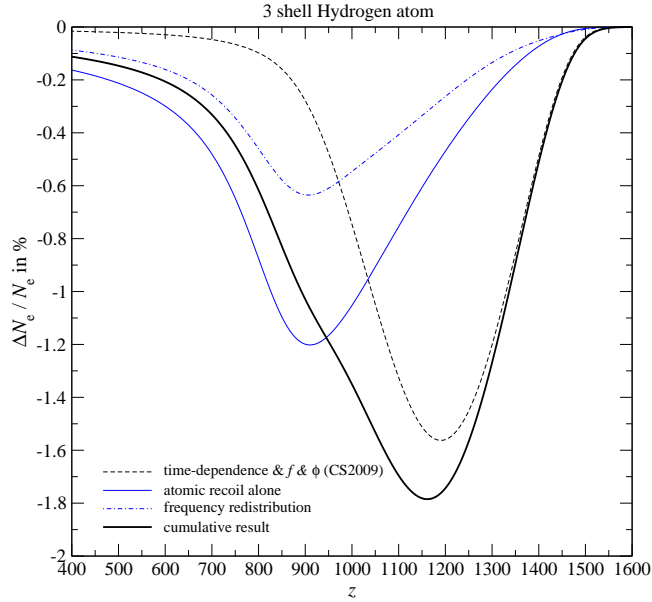


Figure 21: Changes in the free electron fraction due to partial frequency redistribution, including *atomic recoil*, and *Doppler-broadening* and *boosting*. The curve labeled 'CS2009' is the total result from Fig. 20. The figure was taken from Chluba & RS (2009d).

levels or the continuum is given by the CMB blackbody radiation. For example, once an electron reached the 2p-state by the absorption of the Lyman α photon γ_1 , it will only be able to be further excited, say to the 3d-level, by the aid of a Balmer α photon γ_2 from the ambient CMB radiation field. If the energy of the photon γ_1 was initially a bit smaller than the Lyman α frequency, then this lack of energy has to be compensated by the photon γ_2 , since due to energy conservation $\nu_{\gamma_1} + \nu_{\gamma_2}$ should equal the transition frequency to the third shell, ν_{31} . Because during hydrogen recombination blue-ward of the Balmer α resonance there are exponentially fewer photons in the CMB than at the line center, the efficiency of Lyman α absorption is exponentially smaller in the red wing of the Lyman α resonance. With a similar argument, the absorption efficiency is exponentially larger in the blue wing of the Lyman α resonance. This process leads to a $\sim 10\%$ increase in the Lyman α escape probability, and hence speeds hydrogen recombination up. Chluba & RS (2009c) obtained $\Delta N_e / N_e \sim -1.9\%$ at $z \sim 1100$ (see Fig. 20 for more detail).

One should also mention that this large change in the escape probability of Lyman α photons will directly translate into similar changes in the amplitude of the Lyman α line, although the electron fraction was affected by much less. Also, the shape of the low-frequency distortion from highly excited level will be affected by this process, so that the recombination spectrum in principle should allow us to understand the details in the dynamics of hydrogen recombination.

Partial frequency redistribution and its effect on the recombination history

The other key ingredients for the derivation of the escape probability in the Lyman α resonance using the Sobolev approximation (Sobolev, 1960) is the assumption that every line scattering leads to a *complete-redistribution* of photons over the whole line profile. It is clear that this assumption is not very accurate, since in each scattering photons will only be redistributed by $\Delta\nu/\nu \sim 10^{-5} - 10^{-4}$, where the redistribution is related to the Doppler motion of the atom (Hummer, 1962; Rybicki & dell’Antonio, 1993). This again is due to the absence of collisions, since without them a complete redistribution of photons over the Lyman α line profile can only occur when the 2p electron is further excited towards higher levels, forgetting its history on the way. The latter process is related to an absorption event rather than a line scattering. However, during hydrogen recombination the probability for this is about $10^3 - 10^4$ smaller than the scattering rate (e.g. see Chluba & RS, 2008b), so that a complete redistribution becomes rather unlikely in particular when going to the distant line wings, where the total scattering rate is significantly smaller than in the line center (also see explanations in Chluba & RS, 2008b; Switzer & Hirata, 2008a; Chluba & RS, 2009a).

This has lead several groups to consider the frequency redistribution of Lyman α photons in this problem more carefully. Since the Lyman α scattering rate is huge during hydrogen recombination one can use a Fokker-Planck approximation for the redistribution function (e.g. see Rybicki, 2006). Here three processes are important: (i) atomic recoil⁴, (ii) Doppler boosting, and (iii) Doppler broadening. All three physical processes are also well-known in connection with the Kompaneets equation which describes the repeated scattering of photons by free electrons.

Atomic recoil leads to a *systematic drift* of photons towards lower frequencies after each resonance scattering. This allows some additional photons to escape from the Lyman α resonance and thereby speeds hydrogen recombination up, as demonstrated by Grachev & Dubrovich (2008) and others (Chluba & RS, 2009d; Hirata & Forbes, 2009). However, the processes (ii) and (iii) were neglected in the analysis of Grachev & Dubrovich (2008). As recently shown by Chluba & RS (2009d), Doppler boosting acts in the opposite direction as atomic recoil and therefore should slow recombination down, while the effect of Doppler broadening can lead to both an increase in the photons escape probability of a decrease, depending on the initial frequency of the photons (see Chluba & RS, 2009d, for more detailed explanation). The overall correction to the recombination history due to processes (i)-(iii) is dominated by the one caused by atomic recoil effect, and amounts to $\Delta N_e/N_e \sim -0.6\%$ at $z \sim 900$ (see Fig. 21 for more detail). The results of the computations by Chluba & RS (2009d) seem to be in very good agreement with those from Hirata & Forbes (2009).

Finally, in Fig. 22 we show as an example the cumulative effect on the CMB temperature and polarization power spectra caused by the corrections in the ionization history due to *partial frequency redistribution*, the *time-dependent correction*, the *thermodynamic factor*, and the correction due to the *shape* of the effective emission profile. In particular the associated changes in the EE power spectrum are impressive, reaching peak to peak amplitude $\sim 2\% - 3\%$ at $l \geq 1500$. It will be important to take these corrections into account for the analysis of future CMB data.

⁴This term was first introduced by Basko (1978, 1981)

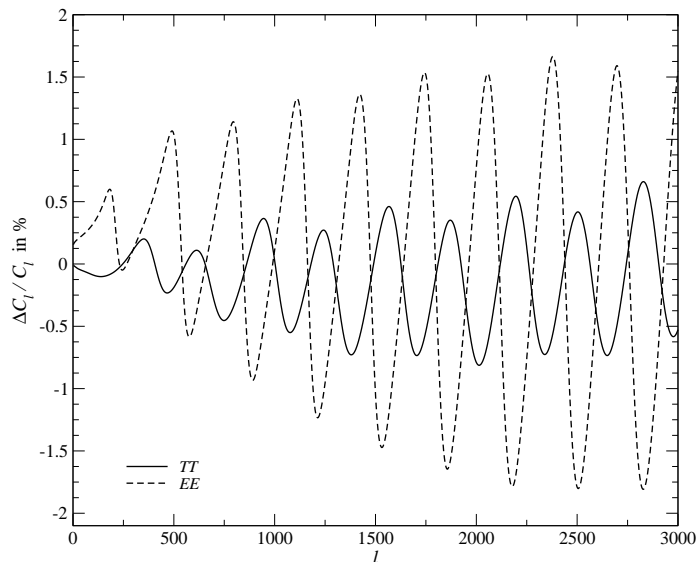


Figure 22: Changes in the CMB temperature and polarization power spectra caused by the cumulative effect of *partial frequency redistribution*, the *time-dependent correction*, the *thermodynamic factor*, and the correction due to the *shape* of the effective emission profile. The figure was taken from Chluba & RS (2009d).

Additional processes during hydrogen recombination

There are a few more processes that here we only want mention very briefly (although with this the list is not meant to be absolutely final or complete). Hirata (2008) also included the *two-photon decays from higher levels* in hydrogen and *2s-1s Raman scattering*. The former lead to an additional speed up of hydrogen recombination at the level of $\Delta N_e/N_e \sim 0.1\% - 0.3\%$, while the Raman process leads to an additional delay of recombination by $\Delta N_e/N_e \sim 0.9\%$ at $z \sim 900$.

The effect of *electron scattering* during hydrogen recombination was also recently investigated by Chluba & RS (2009d) using a Fokker-Planck approach. This approximation for the frequency redistribution function may not be sufficient towards the end of hydrogen recombination, but in the overall correction to the ionization history was very small close the maximum of the Thomson visibility function, so that no big difference are expected when more accurately using a scattering Kernel-approach.

One should also include the small re-absorption of photons from the 2s-1s two-photon continuum close to the Lyman α resonance, where our estimates show that this leads to another $\Delta N_e/N_e \sim 0.1\%$ correction. Also the feedback of helium photons on hydrogen recombination poses an interesting problem, but the changes in the ionization history are negligible (Chluba & RS, 2009e).

3.1 Towards a new recombination code

The list of additional processes that have been studied in connection with the cosmological recombination problem is already very long. However, it seems that most of the important terms have been identified, so that now it is time to think about the inclusion of all these processes in a *new cosmological recombination code*, which then can be used in the analysis of CMB data as will become available with PLANCK soon. The important steps towards this new code will be (i) to *cross validate* all the discussed corrections by independent groups/methods, and (ii) to develop a scheme that is sufficiently *fast* and *precise* and still captures all the important corrections.

The first step is particularly important, since at percent-level accuracy it is very easy to make mistakes, even if they are only due to numerics. For the second point the problem is that one run of the full recombination code will likely take far too long⁵ to be useful for parameter estimation from CMB data. To solve this problem three strategies could be possible: (a) one can find appropriate *fudge functions* to mimic the recombination dynamics using RECFAST; (b) one can try to find an approximate, physically motivated representation of the problem; or (c) one can simply tabulate the outputs of the full recombination code for different cosmologies and then interpolate on the obtained grid of models.

In connection with this we would like to advertise the work of Fendt et al. (2009), leading to the development of RICO⁶, which uses multi-dimensional polynomial regression to accurately represent the dependence of the free electron fraction on redshift and the cosmological parameters. RICO is both very fast and accurate, and can be *trained* using any available recombination code. This feature in addition makes it very interesting in connection with code comparisons and when looking for more approximate, physically motivated representations of the problem. Once we finished our final recombination code we plan on providing the training sets for RICO, so that it then can be used in the data analysis in connection with PLANCK.

4 Conclusions

It took several decades until measurements of the CMB temperature fluctuations became a reality. After COBE the progress in experimental technology has accelerated by orders of magnitude. Today CMB scientists are even able to measure *E*-mode polarization, and the future will likely allow us to access the *B*-mode component of the CMB in addition. Similarly, one may hope that the development of new technologies will render the consequences of the discussed physical processes observable. Therefore, also the photons emerging during the epochs of cosmological recombination could open another way to refine our understanding of the Universe.

As we illustrated in this contribution, by observing the CMB spectral distortions from the epochs of cosmological recombination we can in principle directly measure cosmological parameters like the value of the CMB monopole temperature, the specific entropy, and the pre-stellar helium abundance, *not suffering* from limitations set by *cos-*

⁵In the current implementation our code would take of the order of a week for one cosmology.

⁶<http://cosmos.astro.uiuc.edu/rico>

mic variance. Furthermore, we could directly test our detailed understanding of the recombination process using *observational data*. It is also remarkable that the discussed CMB signals are coming from redshifts $z \sim 1300 - 1400$ for hydrogen, $z \sim 1800 - 1900$ for neutral helium, and $z \sim 6000$ for He II. This implies that by observing these photons from recombination we can actually look beyond the last scattering surface, i.e. before bulk of the CMB temperature anisotropies were actually formed. To achieve this task, *no absolute measurement* is necessary, but one only has to look for a modulated signal at the $\sim \mu\text{K}$ level, with typical amplitude of $\sim 10 - 30 \text{ nK}$ and $\Delta\nu/\nu \sim 0.1$, where this signal in principle can be predicted with high accuracy, yielding a *spectral template* for the full cosmological recombination spectrum, also including the contributions from helium. The combination of both *spectral* and *spatial* fluctuation in the CMB black-body temperature may therefore eventually allow us to perform purely CMB based parameter estimations, yielding competitive constraints on the Universe we live in.

And finally, if something *unexpected* happened *during* or *before* the recombination epoch, then this may leave observable traces in the cosmological recombination radiation. We have illustrated this statement for the case of energy injection in the pre-recombinational epoch (Sect. 2.5), but also if something unexpected occurred during the recombination of hydrogen, e.g leading to *delayed recombination* (Peebles et al., 2000), then this should leave signatures in the cosmological recombination radiation, affecting *not only* the shape of the Lyman α distortion, but also the low frequency part of the recombination spectrum. This might help us to place tighter constraints on the thermal history of our Universe and the physics of cosmological recombination.

References

- Bahcall, N. A., Ostriker, J. P., Perlmutter, S., & Steinhardt, P. J. 1999, *Science*, 284, 1481
- Basko, M. M. 1978, *Zhurnal Eksperimental noi i Teoreticheskoi Fiziki*, 75, 1278
- Basko, M. M. 1981, *Astrophysics*, 17, 69
- Beigman, I. L., & Vainshtein, L. A., in preparation
- Bennett, C. L., et al. 2003, *ApJS*, 148, 1
- Bond, J. R., & Efstathiou, G. 1984, *ApJL*, 285, L45
- Chluba, J., & Sunyaev, R. A. 2006a, *A&A*, 446, 39
- Chluba, J., & Sunyaev, R. A. 2006b, *A&A*, 458, L29
- Chluba, J., & Sunyaev, R. A. 2007, *A&A*, 475, 109
- Chluba, J., Rubiño-Martín, J. A., & Sunyaev, R. A. 2007, *MNRAS*, 374, 1310
- Chluba, J., & Sunyaev, R. A. 2008a, *A&A*, 478, L27
- Chluba, J., & Sunyaev, R. A. 2008b, *A&A*, 480, 629

- Chluba, J., & Sunyaev, R. A. 2009a, *A&A* , 496, 619
- Chluba, J., & Sunyaev, R. A. 2009b, *A&A* , 501, 29
- Chluba, J., & Sunyaev, R. A. 2009c, arXiv:0904.0460
- Chluba, J., & Sunyaev, R. A. 2009d, arXiv:0904.2220
- Chluba, J., & Sunyaev, R. A., in preparation
- Doroshkevich, A. G., Zeldovich, Y. B., & Syunyaev, R. A. 1978, *Soviet Astronomy*, 22, 523
- Drake, G. W. F., & Morton, D. C. 2007, *ApJS* , 170, 251
- Dubrovich, V. K. 1975, *Soviet Astronomy Letters*, 1, 196
- Dubrovich, V. K., & Stolyarov, V. A. 1997, *Astronomy Letters*, 23, 565
- Dubrovich, V. K., & Grachev, S. I. 2005, *Astronomy Letters*, 31, 359
- Eisenstein, D. J., et al. 2005, *ApJ* , 633, 560
- Fendt, W. A., Chluba, J., Rubiño-Martín, J. A., & Wandelt, B. D. 2009, *ApJS* , 181, 627
- Fixsen, D. J., Cheng, E. S., Gales, J. M., Mather, J. C., Shafer, R. A., & Wright, E. L. 1996, *ApJ* , 473, 576
- Fixsen, D. J., & Mather, J. C. 2002, *ApJ* , 581, 817
- Grachev, S. I., & Dubrovich, V. K. 2008, *Astronomy Letters*, 34, 439
- Göppert-Mayer, 1931, *Annalen der Physik*, 9, 273
- Hirata, C. M. 2008, *Phys. Rev. D*, 78, 023001
- Hirata, C. M., & Forbes, J. 2009, arXiv:0903.4925
- Hu, W., Scott, D., Sugiyama, N., & White, M. 1995, *Phys. Rev. D*, 52, 5498
- Hütsi, G. 2006, *A&A* , 449, 891
- Hummer, D. G. 1962, *MNRAS* , 125, 21
- Illarionov, A. F., & Syunyaev, R. A. 1975, *Soviet Astronomy*, 18, 413
- Illarionov, A. F., & Syunyaev, R. A. 1975, *Soviet Astronomy*, 18, 691
- Kholupenko, E. E., Ivanchik, A. V., & Varshalovich, D. A. 2005, *Grav.Cosmol.*, 11, 161
- Kholupenko, E. E., & Ivanchik, A. V. 2006, *Astronomy Letters*, 32, 795
- Kholupenko, E. E., Ivanchik, A. V., & Varshalovich, D. A. 2007, *MNRAS* , 378, L39

Longair, M. S., & Sunyaev, R. A. 1969, *Nature*, 223, 719

Lyubarsky, Y. E., & Sunyaev, R. A. 1983, *A&A* , 123, 171

Madau, P., Meiksin, A., & Rees, M. J. 1997, *ApJ* , 475, 429

Peebles, P. J. E., 1968, *ApJ* , 153, 1

Peebles, P. J. E., & Yu, J. T. 1970, *ApJ* , 162, 815

Peebles, P. J. E. 1982, *ApJL* , 263, L1

Peebles, P. J. E., Seager, S., & Hu, W. 2000, *ApJL* , 539, L1

Perlmutter, S., et al. 1999, *ApJ* , 517, 565

Riess, A. G., et al. 1999, *AJ*, 118, 2675

Readhead, A. 2007, private communication

Rubiño-Martín, J. A., Chluba, J., & Sunyaev, R. A. 2006, *MNRAS* , 371, 1939

Rubiño-Martín, J. A., Chluba, J., & Sunyaev, R. A. 2008, *A&A* , 485, 377

Rybicki, G. B., & dell'Antonio, I. P. 1993, *Observational Cosmology*, 51, 548

Rybicki, G. B. 2006, *ApJ* , 647, 709

Seager, S., Sasselov, D. D., & Scott, D. 1999, *ApJL* , 523, L1

Seager, S., Sasselov, D. D., & Scott, D. 2000, *ApJS* , 128, 407

Silk, J. 1968, *ApJ* , 151, 459

Sobolev, V. V. 1960, *Moving envelopes of stars*, Cambridge: Harvard University Press, 1960

Sunyaev, R. A., & Zeldovich, Y. B. 1970a, *Astrophysics and Space Science*, 7, 3

Sunyaev, R. A., & Zeldovich, Y. B. 1970b, *Astrophysics and Space Science*, 7, 20

Sunyaev, R. A., & Zeldovich, Y. B. 1980, *Ann. Rev. Astron. Astrophys.*, 18, 537

Switzer, E. R., & Hirata, C. M. 2008a, *Phys. Rev. D*, 77, 083006

Switzer, E. R., & Hirata, C. M. 2008b, *Phys. Rev. D*, 77, 083008

Wong, W. Y., Moss, A., & Scott, D. 2008, *MNRAS* , 386, 1023

Vikhlinin, A., et al. 2009, *ApJ* , 692, 1060

Vittorio, N., & Silk, J. 1984, *ApJL* , 285, L39

Zeldovich, Y. B., Kurt, V. G. & Syunyaev, R. A., 1968, *ZhETF*, 55, 278

Zeldovich, Y. B., & Sunyaev, R. A. 1969, *Astrophysics and Space Science*, 4, 301

Zeldovich, Y. B., Rakhmatulina, A. K., & Syunyaev, R. A. 1972, *Radiophysics and Quantum Electronics*, 15, 121